

# REVIEWS OF MODERN PHYSICS

VOLUME 32, NUMBER 1

JANUARY, 1960

## Vibrational States in Deformed Even-Even Nuclei

RAYMOND K. SHELINE\*

*Florida State University, Tallahassee, Florida*

### TABLE OF CONTENTS

I. Introduction.....	1	VI. Potential Energy Surfaces.....	17
II. Analogies between the Correlations in Molecular and in Nuclear Systems.....	3	A. Cases of $\gamma$ and $\beta$ Instability.....	17
A. Similarities.....	3	(1) $\gamma$ Unstable Potential.....	18
B. Differences.....	3	(2) Case of " $\beta$ Instability".....	18
III. Calculations of Vibrational Energies from the Vibration-Rotation Interaction in the Ground State Band.....	4	B. Actual Experimental Situation.....	18
A. Résumé of the Theory.....	4	VII. Discussion of Evidence for Vibrational States in Deformed Even-Even Nuclei.....	18
B. Calculations and Results.....	5	A. Systematic Occurrences of $0+$ and $2+$ Bands and Existence and Nature of Impurities in These Bands.....	19
(1) Calculations.....	5	B. Coulomb-Excitation Cross Sections to Vibrational States in Deformed Nuclei.....	20
(2) Odd $A$ Nuclei.....	7	C. Evidence from the Vibrational States in Spherical Nuclei.....	21
(3) Indications of Success in Calculating $\beta$ and $\gamma$ Vibrations of Even-Even Nuclei.....	7	D. Selection Rules and Other Characteristics of Vibrational States in Deformed Nuclei.....	22
(4) Predictions.....	8	VIII. Conclusion.....	23
(5) Reservations Regarding the Constancy and Meaning of $b$ .....	9	IX. Acknowledgments.....	24
IV. Vibrational and Rotational Level Systematics in the Rare Earths and Actinides.....	9		
A. Positive Parity Levels of Even-Even Nuclei in the Rare Earths and Actinides.....	10		
B. Negative Parity Levels of Even-Even Nuclei.....	11		
V. Interpretation of the Positive Parity Level Systematics.....	12		
A. Relationships between Positive Parity Levels in Deformed and Spherical Nuclei.....	12		
(1) The Graph.....	13		
(2) Energy Relationships between the $0+$ , $2+$ , and $4+$ Members of the Vibrational Bands of Spherical Nuclei.....	13		
(3) Procedure for Constructing " $\beta$ Unstable," $\gamma$ Unstable, and Spherical Nuclear Level Systematics from the Rotational Bands of Deformed Nuclei.....	14		
(4) Problem of Crossing of Levels with the Same Spin and Parity.....	15		
B. Systematics of $\beta$ and $\gamma$ Vibrations.....	16		
(1) Attempt to Explain the Trend in $\gamma$ Vibrations.....	16		
(2) Attempt to Explain the Trend in $\beta$ Vibrations.....	17		

### I. INTRODUCTION

ONE of the most exciting challenges in the study of nuclear structure at the present time is the possibility of a truly unified nuclear model. Such a model must ultimately successfully explain all nuclear spectroscopic data in regions of the nuclear periodic table differing as widely as closed-shell rigid spherical nuclei and deformed nonrigid axially symmetric nuclei. A serious attempt to relate the successful features of the shell model and the collective model has been made recently by Elliott.<sup>1</sup>

<sup>1</sup>J. P. Elliott, "Relation between shell model and rotational model," Proceedings of the Pittsburgh Conference on Nuclear Structure, 298 (June, 1957); Proc. Roy. Soc. (London) **A245**, 128, 562 (1958). *Note added in proof.*—Another way to see the connection between the different nuclear models has recently been pointed out. [See K. Wildermuth and T. Kenelopoulos, Nuclear Phys. **7**, 150 (1958); **9**, 449 (1958/59) and B. F. Bayman and A. Bohr, Nuclear Phys. **9**, 596 (1958/59).] The mathematical description of Elliott is contained in the cluster model, but the cluster model is more general and allows a more physical interpretation. The discussion of collective motion in the framework of the cluster model indicates that the adiabatic condition which is used to differentiate between rotations, vibrations, and single-particle excitations is probably too restrictive.

\* This paper was initiated during a three year term (1955–1958) at the Institute for Theoretical Physics, Copenhagen, Denmark. Support in the form of a research professorship by the Fulbright, Guggenheim, and Ford Foundations, and the Institute for Theoretical Physics itself is gratefully acknowledged.

One of the more serious problems facing such a unified model is the validity of nuclear vibrations. Certain features<sup>2</sup> in spherical even-even nuclei† such as the ratio (approximately 2.2) of the energy of the second excited state to the first excited state, the selection rule against the decay of the second excited state to the ground state, the  $E2$  character of the transition to the first  $2+$  state, and the increasing number of observations of multiplets ( $2+$ ,  $4+$ ) and ( $0+$ ,  $2+$ , and  $4+$ ) for the second excited state are evidence for the interpretation of these states as vibrations. On the other hand, there is a haunting awareness that vibrational energy level spacings are not small compared with single-particle spacings. Accordingly, the vibrations cannot follow the single particle motion as nearly adiabatically as the rotations do. Does this mean that the vibrations are really mixed single-particle vibrational states with position in energy made somewhat random by their relationship to random single-particle states, or have they preserved their identity sufficiently to make it reasonable to call them vibrational states?

This study concerns first, the question of the validity of nuclear vibrations and second, an understanding of the relationships between the collective states in spherical and deformed even-even nuclei. The approach is largely empirical, employing (1) a collection and

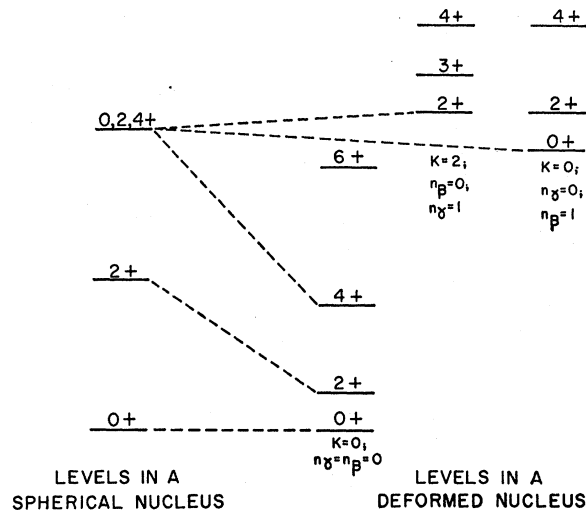


FIG. 1. Relationship between states in spherical and deformed nuclei as deduced from simple comparisons of spins and parity. For more complete relationships see Fig. 9.

<sup>2</sup> G. Scharff-Goldhaber and J. Weneser, Phys. Rev. **98**, 212 (1955); see also M. Nagasaki and T. Tamura, Progr. Theoret. Phys. (Kyoto) **12**, 248 (1954).

† For convenience, nuclei have been classified in this paper as deformed or spherical. Actually, this is probably an oversimplification [see, e.g., the recent papers of Davydov and Filippov, Nuclear Phys. **8**, 237 (1958); **10**, 654 (1959)]. This fact is implicitly recognized in Sec. V.A. (see e.g., Fig. 9), where in addition to rotational and spherical nuclei, “ $\beta$  unstable” and  $\gamma$  unstable nuclei are treated. Accordingly, the term spherical is used in this paper both in the narrow sense where it refers to closed-shell nuclei and in the broader sense in which it refers to all nuclei which do not have simple rotational spectra.

systematization of all experimental rotational and vibrational states in the regions of interest (an attempt has been made to make the data complete to January 1, 1959, with some additional data from January to June 1, 1959), (2) an attempt to calculate additional  $\beta$  and  $\gamma$  vibrations for deformed even-even nuclei, and (3) a summary of the Coulomb excitation of vibrational states whose Coulomb excitation cross sections should be enhanced if these states are really collective in nature. Emphasis is placed on the vibrations of deformed even-even nuclei because more data are available for these nuclei and because the detailed nature of the collective model makes possible not only a calculation for additional vibrations but also a more intricate knowledge and test of observed vibrations. It is hoped that this detailed knowledge of vibrations in the deformed regions may lead to a more intimate knowledge of the immediately neighboring spherical nuclei.

We consider first the collective states of spherical and deformed nuclei and the possible relationships between them. In spherical nuclei<sup>3</sup> removed from closed shells, one expects to find approximately equally spaced vibrational states with the following spin sequence: (1)  $0+$ , (2)  $2+$ , (3)  $0+$ ,  $2+$ ,  $4+$ , etc.; whereas in a deformed nucleus one expects a ground state rotational band with spins  $0+$ ,  $2+$ ,  $4+$ ,  $6+$ , etc.; a  $\gamma$  vibration‡ with a superimposed rotational band with spins  $2+$ ,  $3+$ ,  $4+$ ,  $5+$ , etc.; and a  $\beta$  vibration§ with superimposed rotational band and spins  $0+$ ,  $2+$ ,  $4+$ ,  $6+$ , etc. The level schemes for spherical and deformed nuclei are presented in Fig. 1. Although deformed nuclei have rotational motions which are entirely lacking in spherical nuclei, a relationship is to be expected between the states in spherical and deformed nuclei. In view of the spins and parities of the states involved, it is reasonable to assume that the  $2+$  first vibrational states of spherical nuclei are related to the  $2+$  state of ground state rotational bands of deformed nuclei, that the  $4+$  members of second vibrational states are related to the  $4+$  members of the ground state rotational bands, that the  $2+$  members of the second vibrational states are related to the  $2+$   $\gamma$  vibrational band heads, and that the  $0+$  members of the second vibrational states are related to the  $0+$   $\beta$  vibrational band heads. This relationship is shown in Fig. 1 with dotted lines. One obtains approximately independent harmonic vibrations in the  $\beta$  and  $\gamma$  variables with states labeled  $n_\beta$  and  $n_\gamma$ . A more complete description of the relationships between various types of nuclei is given in Sec. V.A.

The collection of data herein presented showing an innate systematics has obvious empirical value to the experimentalist. It is hoped that the relationships and also the irregularities may have a usefulness for theo-

<sup>3</sup> A. Bohr, Dan. Matt.-Fys. Medd. **26**, No. 14 (1952).

‡ A discussion of  $\beta$  and  $\gamma$  vibrations is given in Sec. III.A. Note added in proof.—Davydov and Filippov, Nuclear Phys. **8**, 237 (1959); **10**, 654 (1959), have proposed a simple way of introducing the  $\gamma$  vibration by considering the nucleus as an asymmetric top.

rists. Thus, although emphasis has been placed on following vibrations from spherical to deformed even-even nuclei, the trend of the  $\gamma$  and  $\beta$  vibrations from spherical to deformed even-even nuclei gives qualitative evidence of the single-particle states in these deformed nuclei. Furthermore, the apparent success in calculating the  $\gamma$  and  $\beta$  vibrations in deformed even-even nuclei has theoretical implications for the type of collective model to be used in understanding rotation-vibration interaction in deformed nuclei. Finally, the suggested correlations presented here could serve as a guide for a formal theory of intermediate coupling. Such a theory at its two extremes (strong and weak coupling) should reproduce the characteristic spectra of deformed and spherical nuclei, respectively (Fig. 1), but otherwise should reproduce the nuclei of the transition region, e.g., Os<sup>190</sup>, which have characteristics intermediate between spherical and deformed nuclei. A paper discussing this intermediate situation is being prepared.<sup>4</sup>

## II. ANALOGIES BETWEEN THE CORRELATIONS IN MOLECULAR AND IN NUCLEAR SYSTEMS

### A. Similarities

The correlation diagrams of collective states are to a considerable extent self-justifying and, by the very presence of smooth trends in energy *vs* neutron and/or proton number, imply a theoretical significance. Thus, just as one finds that the rotational constants of the CO<sub>2</sub><sup>+</sup> and CO<sub>2</sub> molecules are very similar, so one finds the rotational constants of two nuclei differing by two neutrons, e.g., Hf<sup>178</sup> and Hf<sup>180</sup>, to be very similar.

In some sense one must think of the electron in the case of the CO<sub>2</sub><sup>+</sup>—CO<sub>2</sub> system and the two neutrons in the case of the Hf<sup>178</sup>—Hf<sup>180</sup> system as affecting very little the bulk properties of their respective systems. In the case of the CO<sub>2</sub><sup>+</sup>—CO<sub>2</sub> system, the electron does not affect very much the interatomic distance and hence the moment of inertia. Likewise, in the case of the Hf<sup>178</sup>—Hf<sup>180</sup> system, the deformation and the moment of inertia are largely unaffected. This analogy is shown in Table I. Therefore, just as there is a considerable theoretical significance to the correlations of collective effects between molecular systems like CO<sub>2</sub><sup>+</sup> and CO<sub>2</sub>,<sup>5</sup> one might expect correlations between collective motions of even-even nuclei differing by 2, 4, 6, ... neutrons or protons to have a theoretical significance. Although no attempt is made to suggest a formal procedure by which the experimentally observed correlations can be theoretically explained, a qualitative descriptive attempt to explain the correlations for  $\gamma$  vibrations is undertaken.

If the addition of two neutrons or two protons produces a basic change in the geometry of the system, one must expect a disruption in the trend of the correlations. This is the case, for example, when one changes

TABLE I. Comparison between nuclear and molecular systems of the rotational constants of CO<sub>2</sub> and CO<sub>2</sub><sup>+</sup> and of Hf<sup>178</sup> and Hf<sup>180</sup>.

Molecules	Molecular systems		Nuclear systems	
	Moment of inertia $I_0(10^{-40} \text{ g/cm}^2)$	Interatomic distance $r_0(10^{-8} \text{ cm})$	Moment of inertia $3\hbar^2/\beta$ (kev)	Deformation nucleus ( $\beta$ )
CO <sub>2</sub> <sup>a</sup>	71.87	1.1632	91	0.31 Hf <sup>178</sup> <sup>c</sup>
CO <sub>2</sub> <sup>+</sup> <sup>b</sup>	73.55	1.1767	66	0.27 Hf <sup>179</sup> <sup>c</sup>
			93	0.27 Hf <sup>180</sup> <sup>c</sup>

<sup>a</sup> G. Herzberg, Revs. Modern Phys. **14**, 219 (1942).

<sup>b</sup> S. Mrozowski, Phys. Rev. **60**, 730 (1941); **62**, 270 (1942).

<sup>c</sup> Reference 10.

from 88 to 90 neutrons.<sup>6</sup> In this case the nucleus changes from a spherical to a deformed nucleus. The two additional neutrons are obviously involved in a change much more drastic than those involving the bulk properties of the nucleus. As in a molecular system, in which the addition or subtraction of an electron produces a change in the geometry, one can expect an alteration in the trend of the constants for collective motion.

### B. Differences

There are considerable differences between simple molecular systems and nuclear systems. Thus, whereas the CO<sub>2</sub><sup>+</sup>—CO<sub>2</sub> systems differ by only one electron, Hf<sup>178</sup> and Hf<sup>180</sup> differ by two neutrons. If one chose to compare the low energy states of Hf<sup>179</sup> with either Hf<sup>178</sup> or Hf<sup>180</sup>, the comparison would not be so obvious. This difficulty arises because even-even nuclei develop a gap between the ground state and higher excited states. This gap is of the order of 1–2 Mev in the rare earth region. In this region the collective motions (vibrations and rotations for deformed nuclei) are allowed to develop freely on the 0+ state. There is no corresponding gap in the odd *A* nuclei. Consequently, rotational and vibrational states must compete with intrinsic states for prominence in the low-energy spectrum. Furthermore, the moment of inertia of the odd *A* nucleus is, in general, considerably less than for the neighboring even *A* nuclei (see Table I). This difference has been ascribed<sup>7</sup> to the difference in level spacing in even-even and odd *A* nuclei. The general occurrence of considerably lower intrinsic states in odd *A* nuclei implies that the intrinsic motion cannot follow the rotational motion adiabatically. This results in a corresponding increase in the moment of inertia for odd *A* nuclei. Accordingly, the correlation diagrams for vibrations and rotations presented in this paper compare even-even nuclei only.

In the second place, correlations in molecular systems involve only changes in the number of electrons in the systems compared, whereas correlations in nuclear systems involve changes in the number of either neutrons or protons or both. This results in considerably

<sup>4</sup> D. Bes and R. K. Sheline (in preparation).

<sup>5</sup> R. S. Mulliken, J. Chem. Phys. **3**, 720 (1935).

<sup>6</sup> B. R. Mottelson and S. C. Nilsson, Phys. Rev. **99**, 1615 (1955).

<sup>7</sup> A. Bohr and B. R. Mottelson, Dan. Matt. Fys. Medd. **30**, No. 1, (1955).

greater complexity in nuclear correlations. Although the difference is only a formal one, it results in practical difficulties in presenting nuclear correlations.

### III. CALCULATIONS OF VIBRATIONAL ENERGIES FROM THE VIBRATION-ROTATION INTERACTION IN THE GROUND STATE BAND

Since the experimental data on  $\beta$  and  $\gamma$  vibrations of deformed nuclei are so incomplete, we attempt to develop a method of calculating these vibrational energies before presenting the correlations in energy levels. We follow the development of Bohr and Mottelson.<sup>8,9</sup>

#### A. Résumé of the Theory

The low-energy excitations of deformed nuclei expected in the regions far from closed shells are (1) intrinsic, (2) vibrational, and (3) rotational. Most characteristic and therefore easily identifiable are the rotations. The rotations of an axially symmetric deformed nucleus may be characterized by the quantum numbers  $I$ ,  $K$ , and  $M$ , where  $K$  and  $M$  are the components of  $I$  on the intrinsic symmetry axis and on the space-fixed symmetry axis, respectively. Thus, the coupling scheme and the rotational spectra are similar to those of linear molecules. The form of this rotational spectrum is to first order<sup>10</sup>

$$E_I = E_0 + \hbar^2/2\mathcal{I} \{ I(I+1) + a(-1)^{I+\frac{1}{2}}(I+\frac{1}{2})\delta_{K,\frac{1}{2}} \}, \quad (\text{III.1})$$

where  $E_0$  is a constant depending only on the intrinsic structure,  $\mathcal{I}$  is the moment of inertia perpendicular to the nuclear symmetry axis, and the last term involving  $a$ , the decoupling parameter, is present only for  $K = \frac{1}{2}$  states. It is convenient to write  $\epsilon = \hbar^2/2\mathcal{I}$ .

For even-even nuclei in which the ground state has  $I=K=0$ , an especially simple type of rotational spectrum occurs. The rotational states have  $I=0+$ ,  $2+$ ,  $4+$ ,  $\dots$ , even parity, and  $K=0$ . Equation (III.1) predicts that

$$\begin{aligned} (E_4 - E_0)/(E_2 - E_0) &= 3.333, \\ (E_6 - E_0)/(E_2 - E_0) &= 7.000, \\ (E_8 - E_0)/(E_2 - E_0) &= 12.000, \text{ etc.} \end{aligned}$$

The successful prediction of these ratios is one of the great successes of the collective model. However, second-order terms imply deviations from Eq. (III.1). Some of these deviations have the same  $I$  dependence as Eq. (III.1). This results only in corrections to the moment of inertia. Others, however, are analogous to

<sup>8</sup> A. Bohr and B. R. Mottelson, Dan. Matt. Fys. Medd. **27**, No. 16 (1953).

<sup>9</sup> A. Bohr and B. R. Mottelson, *Beta and Gamma Ray Spectroscopy* (North-Holland Publishing Company, Amsterdam, 1955), Chap. 17.

<sup>10</sup> Alder, Bohr, Huus, Mottelson, and Winther, Revs. Modern Phys. **28**, 432 (1956).

the rotation-vibration interaction in molecules<sup>11,12</sup> and involve higher powers of  $I$ . This produces a distortion of the spectrum, lowering these ratios of rotational-state energy intervals. Just as in molecules, where this distortion implies a centrifugal stretching, so in nuclei it implies an increase in  $\beta$  with increasing  $I$  due to centrifugal stretching.

We now consider the questions, (1) What vibrations are to be expected in deformed nuclei, and (2) Is it possible to calculate their energy above the ground state from the distortion of the ground state rotational spectrum resulting from the rotation-vibration interaction?

Deformed axially symmetric nuclear vibrations may be characterized by the quantum number  $\lambda$ , corresponding to the multipole order for small nuclear eccentricities [the parity of the vibration is given by  $(-1)^\lambda$ ], and by  $\nu$ , corresponding to the component of vibrational angular momentum around the symmetry axis. The lowest lying vibrations<sup>10</sup> of a deformed axially symmetric nucleus are quadrupole vibrations which separate into two modes, one with  $\nu=0$  ( $\beta$  vibration) and one with  $\nu=2$  ( $\gamma$  vibration) (see e.g., Fig. 1).  $\nu=\pm 1$  can be shown to be the same as a rotation.

Thus the  $\beta$  vibration, having  $K=0$ , is an axially symmetric vibration similar to the "breathing mode" in molecules in which the eccentricity of the ellipsoid of revolution changes. In the  $\gamma$  vibration the axial symmetry is destroyed,  $K=2$ ; that is, if one looks along the symmetry axis, the outline is an ellipse.

The  $\beta$  and the  $\gamma$  vibrations affect the pure rotation spectrum of Eq. (III.1) by the addition of a rotation-vibration interaction term which is given to first order as<sup>8</sup>

$$\Delta E_\beta = -\frac{3}{2}(1/\hbar\omega_\beta)^2 \epsilon^2 I^2 (I+1)^2, \quad (\text{III.2})$$

$$\Delta E_\gamma = -\frac{1}{2}(1/\hbar\omega_\gamma)^2 \epsilon^2 I^2 (I+1)^2, \quad (\text{III.3})$$

where  $\hbar\omega_\gamma$  and  $\hbar\omega_\beta$  are the energies of the  $\beta$  and  $\gamma$  vibrations, respectively.

If one chooses not to differentiate between the  $\beta$  and  $\gamma$  vibration, the rotation-vibration interaction term to first order is

$$\Delta E_T = \Delta E_\beta + \Delta E_\gamma = -2(1/\hbar\omega_{\text{vib}})^2 \epsilon^2 I^2 (I+1)^2, \quad (\text{III.4})$$

where  $\hbar\omega_{\text{vib}}$  is the energy of a hypothetical single nuclear vibration.

If we now rewrite Eq. (III.1) considering only even-even nuclei and therefore dropping the term in  $a$ , dropping the constant  $E_0$ , since all energies are measured relative to the ground state, but adding an additional term in  $I^2(I+1)^2$  expressive of the rotation-vibration interaction, we have for the ground state rotational band

$$E = \frac{1}{2}\epsilon I(I+1) - BI^2(I+1)^2. \quad (\text{III.5})$$

<sup>11</sup> G. Herzberg, *Molecular Spectra and Molecular Structure I* (D. Van Nostrand Company, Inc., Princeton, New Jersey, 1950).

<sup>12</sup> H. H. Nielsen, Revs. Modern Phys. **23**, 90 (1951).

We may now relate the rotation-vibration interaction energies of Eqs. (III.2) and (III.3) or of (III.4) to the term in  $I^2(I+1)^2$  of Eq. (III.5). When this is done we can solve explicitly for  $\hbar\omega_\beta$ ,  $\hbar\omega_\gamma$ , and  $\hbar\omega_{\text{vib}}$ :

$$\hbar\omega_\beta = \left[ \frac{\frac{3}{2}\epsilon^3}{B - \frac{1}{2}\epsilon^3/(\hbar\omega_\gamma)^2} \right]^{\frac{1}{2}}, \quad (\text{III.6})$$

$$\hbar\omega_\gamma = \left( \frac{\frac{1}{2}\epsilon^3}{B - \frac{3}{2}\epsilon^3/(\hbar\omega_\beta)^2} \right)^{\frac{1}{2}}, \quad (\text{III.7})$$

$$\hbar\omega_{\text{vib}} = (2\epsilon^3/B)^{\frac{1}{2}}. \quad (\text{III.8})$$

## B. Calculations and Results

### (1) Calculations

By using the 2+ and 4+ states of the ground state rotational band of even-even nuclei, it is possible to calculate  $\epsilon = \hbar^2/2\mathcal{I}$  and  $B$  of Eq. (III.5) for all nuclei in which these states are known. The resulting values of  $B$  are shown in columns 7 and 8 of Table II and columns 5 and 6 of Table III. The values of  $B$ , like the energies of the ground state rotational band, when plotted against neutron number, proton number, or atomic number, show an unsymmetrical but relatively smooth trend with largest values in the regions of transition between spherical and spheroidal nuclei. Such a plot against neutron number is shown in Fig. 2. It is obvious that there is also a proton dependence and that a three-dimensional plot would lead to a smooth surface. In view of the smoothness of the plot, it is conceivable that a calculation of the vibrational energies using the values of  $B$  and formulas (III.6), (III.7), or (III.8) might lead to a smooth trend in the vibration energies.

However, before carrying out such calculations it is well to see whether this type of calculation can give even approximately the right energy for the vibration. If one takes  $B$  values from the middle of the rare earth region of deformation, e.g., Lu<sup>172</sup> or Hf<sup>180</sup>, one finds that the calculated vibrational energy is  $\sim 2.2$  and  $\sim 2.1$  Mev, respectively. Such energies need not mean that both the  $\beta$  and  $\gamma$  energy are approximately 2.2 Mev, but if the  $\beta$  vibration energy is lower than 2.2 Mev the  $\gamma$  must be higher, and if the  $\gamma$  is lower than 2.2 the  $\beta$  must be higher. Since there are no experimentally known  $\gamma$  vibrational energies as high as 1.25 Mev and no experimentally known  $\beta$  vibrational energies as high as 1.7 Mev, it appears that the method of calculation as outlined is not satisfactory.

An alternative procedure would involve the use of a nucleus which had both a well-established ground state rotational band and established  $\beta$  and  $\gamma$  vibrational bands. The value for  $B$  [Eq. (III.5)] could be calculated. It could then be adjusted by a factor  $b$  which would reproduce the established  $\beta$  or  $\gamma$  vibrations by the use of Eqs. (III.6) and (III.7) in which  $B$  is replaced by  $bB$ . Once this factor  $b$  is determined it would be

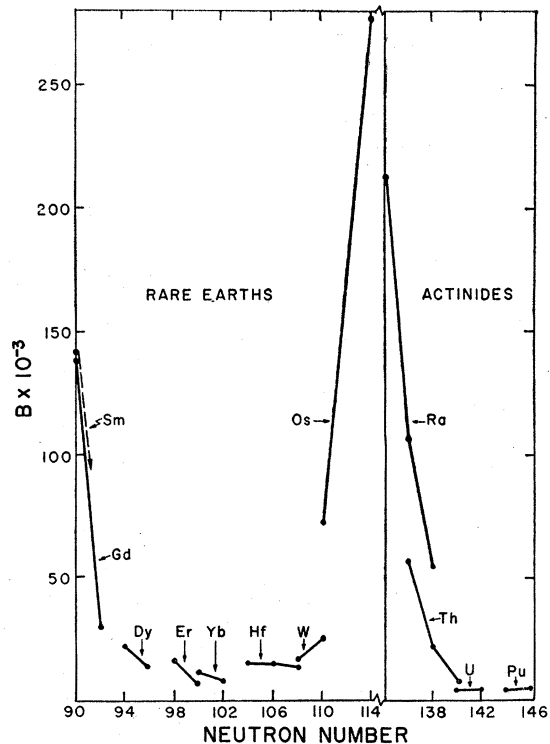


FIG. 2. A plot of the vibration-rotation interaction, namely,  $B \times 10^{-3}$  [see Eq. (III.5)] versus neutron number in the rare earth and actinide regions of deformed nuclei. The vibration-rotation interactions mirror, to a considerable extent, the energy of the first excited state.

hoped that it would be approximately constant from nucleus to nucleus so that one could calculate the position in energy of  $\beta$  and  $\gamma$  vibrations from the vibration-rotation interaction in the ground state band.

At the time these calculations were undertaken, the only nucleus with well-established ground state rotational band and  $\beta$  and  $\gamma$  vibrations were Pu<sup>238</sup>. The levels are shown in Fig. 3.<sup>13,14</sup> The energy values for the Pu<sup>238</sup> ground state rotational band are taken as the average of two precision measurements<sup>15,16</sup> in the decay of Cm<sup>242</sup> and Np<sup>238</sup>. In this way a value for  $B$  of  $3.32 \times 10^{-3}$  is calculated. Then, by using Eqs. (III.6) and (III.7), it is found that this value of  $B$  is too small by a factor of 2.12, which therefore becomes the value of  $b$ . This indicates that the vibration-rotation interaction in the ground state band of Pu<sup>238</sup> and the resulting deviation from a simple  $I(I+1)$  relation produced by the presence of experimentally proven  $\beta$  and  $\gamma$  vibrations is less by the factor 2.12 than that predicted by the hydrodynamical model.

<sup>13</sup> R. G. Albridge and J. M. Hollander, University of California Radiation Laboratory Rept. UCRL-8034 (November, 1957) (unpublished).

<sup>14</sup> I. Perlman and J. O. Rasmussen, *Handbuch der Physik* (Springer-Verlag, Berlin, 1957), Vol. 42.

<sup>15</sup> W. G. Smith and J. M. Hollander, *Phys. Rev.* **101**, 746 (1956).

<sup>16</sup> S. A. Baranov and K. N. Shlyagin, *Atomnaya Energ.* **1**, 52 (1956).

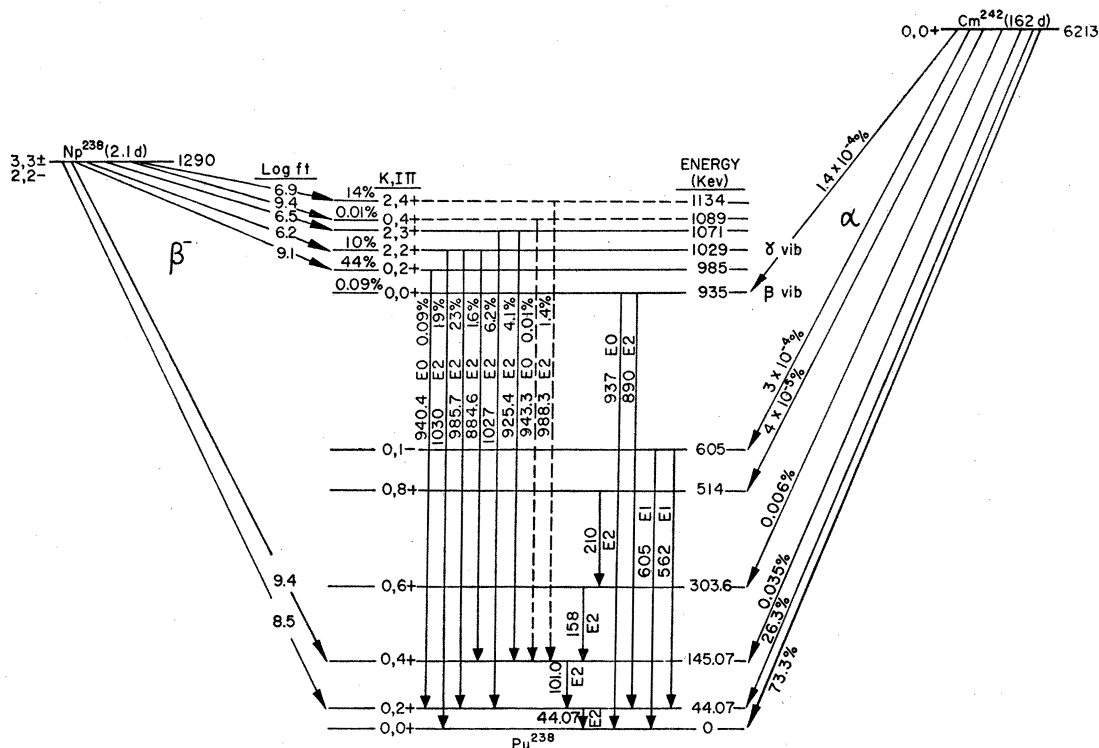


FIG. 3. Energy levels of  $\text{Pu}^{238}$  as determined in the  $\beta^-$  decay of  $\text{Np}^{238}$  and the  $\alpha$  decay of  $\text{Cm}^{242}$  (see references 13 to 16).

In Table II the value of  $B$  calculated for the ground state rotational band of nuclei which have known  $\beta$  or  $\gamma$  vibrational bands is used together with the assumed constant  $b=2.12$  to calculate the energy of the  $\gamma$  or  $\beta$  vibrational band by using Eqs. (III.6) and (III.7). These calculated energies are listed in columns 9 and 10 of Table II.

In Table III the same calculations are carried out for nuclei which have a well-established ground state rotational band but no experimentally observed vibrational bands. It is possible to calculate a single hypothetical nuclear vibration by using the factor  $b=2.12$  which would produce the observed vibration-rotation interaction in the ground state rotational band. The energy

TABLE II. Rotational constants for the ground state bands of nuclei, and calculation of vibrational levels. Only those nuclei are treated in which either a  $\beta$  or a  $\gamma$  vibration or both are experimentally known.

1	2			3	4	5	6	7	8	9	10
Nucleus	Ground state rotational band					Exptl. obs	Exptl. obs	$\hbar^2/2I$ <sup>a</sup>	$B \times 10^{-3}$ <sup>a</sup>	Calc <sup>b</sup>	Calc <sup>b</sup>
	2+(kev)	4+(kev)	6+(kev)			$\gamma$ vib	$\beta$ vib	(kev)		$\gamma$ vib	$\beta$ vib
						2+(kev)	0+(kev)			(kev)	(kev)
$\text{Sm}^{152}$	121.79	366.39				1086		42.29	141.36	...	651
$\text{Gd}^{154}$	123.07	371.07				998		42.70	139.86	...	674
$\text{Gd}^{156}$	88.97	288.2	584.9			1152		30.02	29.89	...	874
$\text{Dy}^{160}$	87.0	284				964		29.26	21.43	...	1084
$\text{Er}^{166}$	80.85 <sup>c</sup>	265.1 <sup>c</sup>	554.1 <sup>c</sup>				$\sim 1450$	27.14	15.71	728	...
$\text{W}^{182}$	100.09	329.36	680.38			1221.8		33.55	15.25	...	1695
$\text{W}^{184}$	111.20	364.04				903.3		37.35	23.68	...	2329
$\text{Os}^{186}$	137.2	437	868.9			768		46.62	72.60	...	1484
$\text{Os}^{188}$	154.9	478				633	(1086)	<sup>d</sup>	<sup>d</sup>	...	<sup>d</sup>
$\text{Os}^{190}$	188	547	1047			557		65.65	276.18 <sup>e</sup>	...	1810
$\text{Th}^{228}$	57.8	186.6	371.6			966		19.53	21.64	...	517
$\text{U}^{234}$	43.25	143.05	296.15				803	14.47	4.00	1029	...
$\text{Pu}^{238}$	44.07 <sup>f</sup>	145.07	303.59			1029	935	14.73	3.32	(1029) <sup>g</sup>	(935) <sup>g</sup>

<sup>a</sup> These are determined by using 2+ and 4+ states only and Eq. (III.5). When 6+ or 8+ states are known, in general their accuracy is not as good as the lower energy rotational states.

<sup>b</sup> Calculated by using the factor  $b=2.12$  times the  $B$  of column 8 and Eqs. (III.6) or (III.7).

<sup>c</sup> Energies for the 2+ and 4+ states are determined by averaging the internal conversion lines of Mihelich *et al.*<sup>19</sup> and Gromov *et al.*<sup>18</sup> Energy for the 6+ state is determined from the average for the 4+ state plus the 6+  $\rightarrow$  4+ 28-kev transition.

<sup>d</sup> The value for the energy of the 4+ state was not known accurately enough at the time these calculations were made to compute these numbers.

<sup>e</sup> The  $\text{Os}^{190}$  ground state rotation spectrum is not a good rotational spectrum. Nonetheless, the  $V$  value (column 8) is calculated in the usual way by using the 2+ and 4+ states only.

<sup>f</sup> Average of the two most accurate conversion electron energy determinations.

<sup>g</sup> Used to determine the factor  $b=2.12$ .

TABLE III. Rotational constants for the ground state bands of nuclei, and estimation of vibrational energies when possible. No  $\beta$  or  $\gamma$  vibrations have been observed in these nuclei.

1	2	3	4	5	6	7	7	9
Nucleus	Ground state rotational band			$\hbar^2/g^a$ (keV)	$B \times 10^{-3}^a$	$\hbar\omega_{\text{vib}}^b$ (keV)	Est. <sup>c</sup> or calc $\gamma$ vib (keV)	Est. <sup>c</sup> or calc $\beta$ vib (keV)
	2+(keV)	4+(keV)	6+(keV)					
Dy <sup>162</sup>	80.8	265.6		27.09	13.32	1187	1026	(1260)
Er <sup>168</sup>	79.9	264.5		26.71	6.54	1658	...	...
Yb <sup>170</sup>	84.2	277.7		28.19	10.61	1411	...	...
Yb <sup>172</sup>	78.7	260.2		26.32	7.61	1504	...	...
Hf <sup>176</sup>	88.3	290.4		29.60	14.04	1423	(1240)	1351
Hf <sup>178</sup>	93.2	306.9		31.26	14.18	1425	(1310)	1471
Hf <sup>180</sup>	93.3	309.3		31.26	13.21	1476	(1270)	1572
Ra <sup>222</sup>	111	310	641.3 <sup>d</sup>	39.57	214.29	522	(900)	473
Ra <sup>224</sup>	84.45	251.45		29.44	107.32	474	(860)	417
Ra <sup>226</sup>	67.62	210.0	416.0	23.20	55.00	463	(850)	417
Th <sup>226</sup>	72.1	226.4	456.4	24.91	56.78	507	(960)	455
Th <sup>230</sup>	52.8	173.8		17.69	7.86	816	(970)	754
U <sup>232</sup>	47.2	156.3	321	15.78	3.68	1003	...	...
Pu <sup>240</sup>	42.87	141.77		14.34	4.04	829	...	...

<sup>a</sup> Values determined by using 2+ and 4+ states only and Eq. (III.5). When 6+ or 8+ states are known, their accuracy is, in general, not as good as the 2+ and 4+ states.

<sup>b</sup> Calculated by using the factor  $b=2.12$  times the  $B$  of column 6 and Eq. (III.8).

<sup>c</sup> When it is possible from the trends of vibrations of neighboring nuclei to estimate a vibration, this is listed in parentheses. The other vibration is then calculated by using the factor  $b=2.12$  times the  $B$  of column 6 and Eqs. (III.6) and (III.7).

<sup>d</sup> Not very accurately known.

for this nuclear vibration calculated by using Eq. (III.8) is listed in column 6 of Table III. Fortunately, in the majority of cases it is possible to estimate the position of either the  $\beta$  or  $\gamma$  vibrational band from the systematics of these bands in neighboring nuclei. When this is done, the assumed energy is listed in parentheses. It is then possible to calculate the position of the other band. These calculated and assumed bands are listed in columns 8 and 9 of Table III and must be considered quite tentative.

### (2) Odd $A$ Nuclei

Odd  $A$  nuclei always have a nonvanishing momentum which must be coupled with the angular momentum of the collective degrees of freedom. There is the additional complexity of other low-lying single-particle states. As previously explained, this competition between vibrational and single-particle states both decreases the probability of the experimental observation of vibrational states in odd  $A$  nuclei and decreases the probability that they would be recognizable because of the increased Coriolis mixing between single-particle states. Finally, there is the fact that one expects two  $\gamma$  vibrational bands,  $\gamma_1=K_0+2$  and  $\gamma_2=K_0-2$ . Thus, one expects three vibrational bands in odd  $A$  nuclei. Although no vibrations in odd  $A$  nuclei have been experimentally observed, it is possible to calculate the energies for such vibrations with the same assumptions which were used for even-even nuclei. As an example we can choose the precision spectroscopy<sup>17</sup> on the Coulomb excited rotational states of Tb<sup>159</sup> and Ho<sup>165</sup>. By using the experimentally observed states, 57.99 and 137.49 keV in Tb<sup>159</sup> and 94.69 and 204.61 keV in Ho<sup>165</sup>, one calculates  $\hbar^2/g=23.36$  and  $B=11.27 \times 10^{-3}$  for Tb<sup>159</sup> and

$\hbar^2/g=23.18$  and  $B=26.41 \times 10^{-3}$  for Ho<sup>165</sup>. Reference to Tables II and III seems to indicate that these  $B$  values are normal and are comparable to the  $B$  values computed for neighboring even-even nuclei. If one uses the value  $b=2.12$ , vibrational energies of 746 keV (Ho<sup>165</sup>) and 1155 keV (Tb<sup>159</sup>) result. Ho<sup>165</sup> (ground state spin 7/2) should have three vibrational bands whereas Tb<sup>159</sup> (ground state spin 3/2) should have only two. This seems to indicate that one may expect to find odd  $A$  vibrations in roughly the same place they are to be found in even-even nuclei. Although a careful experimental search for these levels seems worthwhile, perturbation effects of the type discussed by Kerman using W<sup>183</sup> as an example [see, e.g., A. K. Kerman, Kgl. Danske Videnskab. Selskab, Mat. fys. Medd. **30**, No.15 (1956)] may overshadow the rotation-vibration interaction and thereby invalidate these predictions.

### (3) Indications of Success in Calculating $\beta$ and $\gamma$ Vibrations of Even-Even Nuclei

The single most direct verification of this method of calculating vibrational frequencies involves the levels of Ho<sup>166</sup>. Recently, Gromov *et al.*<sup>18</sup> have studied the decay of Tm<sup>166</sup>. Although they have not published a decay scheme, using their data together with that of other investigators, it is possible to construct the level scheme for Ho<sup>166</sup> as shown in Fig. 4. § The presence of a  $\gamma$  vibration at 787.4 keV in addition to the previously

<sup>18</sup> Gromov, Dscelepov, Dmitriev, Morozov, Peker, and Preobrasenskij, Program and Abstracts of the VIIIth Annual Meeting on Nuclear Spectroscopy (January, 1958), p. 28.

§ Since the completion of this paper Jacob *et al.* [Jacob, Mihelich, Harmatz, and Handley, Bull. Am. Phys. Soc. Ser. II, **3**, 358 (1958)] have published a decay scheme similar to that in Fig. 4. We have used the average of their values and those of Gromov *et al.*<sup>18</sup> for the ground state band but have used the values of Jacob *et al.* for the  $\gamma$  vibrational band except for the  $K=2$ , 5+ state which is not present in their scheme.

<sup>17</sup> Chupp, Dumond, Gordon, Jopson, and Mark, Bull. Am. Phys. Soc. Ser. II, **3**, 268 (1958).

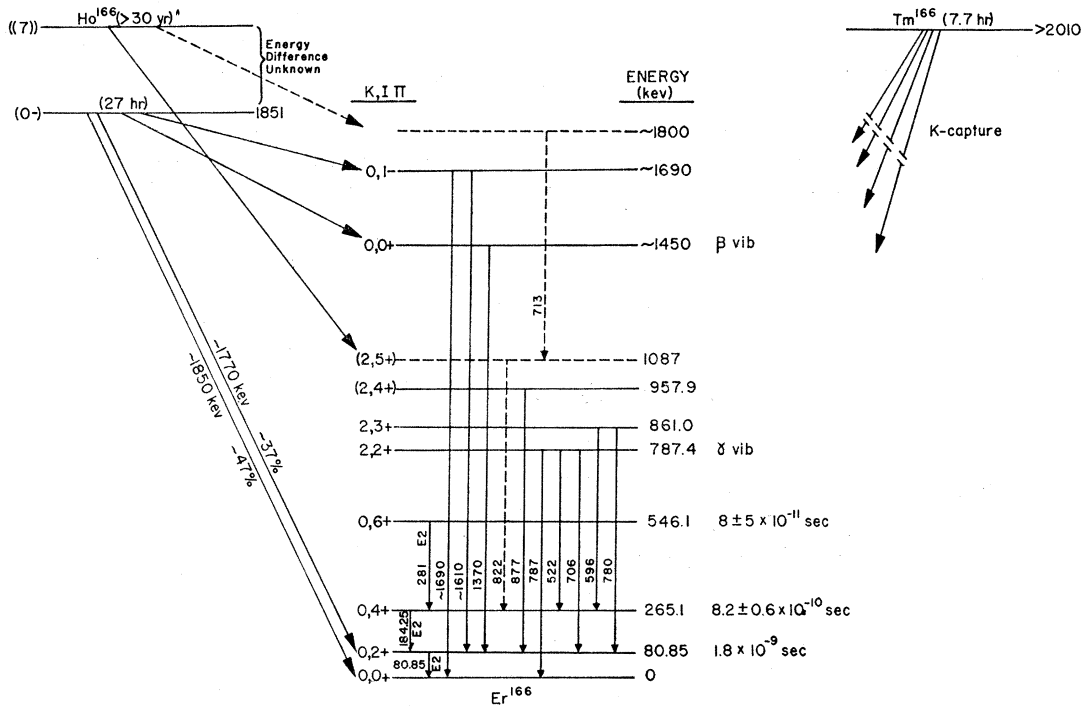


FIG. 4. Energy levels of  $\text{Er}^{166}$  as determined in the  $K$ -capture decay of  $\text{Tm}^{166}$  and the  $\beta^-$  decay of  $\text{Ho}^{166}$ . The first three excited states are averages of the work of references 18 and 19. More recently, Jacob *et al.* [Bull. Am. Phys. Soc. II 3, 358 (1958)] have suggested a similar decay scheme.

observed  $\beta$  vibration at 1450 keV makes it possible to test the validity of the method of calculating vibrations. By using the ground state rotational band measured by Mihelich *et al.*,<sup>19</sup> and the value of  $b=2.12$ , one calculates 875 keV for the  $\gamma$  vibrational band. By using the slightly different measurements of the ground-state band of Gromov *et al.*,<sup>18</sup> one calculates 638 keV. If one averages the two measurements of the ground-state rotational band, one calculates 728 keV as listed in Table II. The frequencies calculated from the two different sets of measurements of the ground state rotational band bracket the experimentally observed frequency. The calculation also indicates the extreme sensitivity of the method to the energies of the ground state band especially as in this case when the  $B$  value is small.

Although not as direct, perhaps the most convincing argument for this method of calculating vibrational energies is the general agreement between calculated energies and the experimentally observed energies of neighboring nuclei. This agreement is most graphically shown in Figs. 5 and 6, where experimental and calculated energies for the vibrations are indicated by using different kinds of points. The general agreement between these points is obvious at once. In general, the agreement is so good that energies of the ground state bands of the few disagreements are suspect. Thus, the ground state bands of  $\text{Er}^{168}$ ,  $\text{Ra}^{222}$ ,  $\text{U}^{232}$ , and  $\text{Pu}^{240}$  would bear additional measurements. Even in these cases

<sup>19</sup> Mihelich, Harmatz, and Handley, Phys. Rev. 108, 989 (1957).

present measurements are not seriously in error and in all cases except  $\text{Ra}^{222}$  very small changes in the ground state band can produce big relative changes in the value of  $B$ . There are two sets of measurements for the ground state band of  $\text{Ra}^{226}$  which differ somewhat. These calculations indicate that 67.62, 210.0, and 416.0 keV rather than 67.8, 208.8, and 414.8 keV are to be preferred for the ground-state band of  $\text{Ra}^{226}$ .

#### (4) Predictions

Since it is possible to calculate vibrational levels that are thus far experimentally unobserved, the success of the prediction of these levels will provide the best test of the method. In spite of the simplicity of the calculation method [see Sec. III.B (5)], if predictions are to be applied as a test, then calculated frequencies must be expected to be approximately correct. However, those cases in which  $B$  is large offer the best test, since the method is not exposed to such serious difficulties in the form of small experimental errors in measurements of the ground state rotational band. Also, the predictions for  $\text{Os}^{190}$ , must be suspect in spite of a large  $B$  value, since this  $B$  value cannot reduce the higher levels to a simple  $I(I+1)$  dependence. Therefore, the best test of the method is the predicted frequencies of  $\text{Sm}^{152}$  (651 keV and  $\text{Gd}^{154}$  (674 keV) (probably  $\text{Nd}^{150}$ , also a 90-neutron nucleus, also has a  $\beta$  vibration in the vicinity of 660 keV) and the  $\beta$  vibrations of  $\text{Ra}^{222}$ ,  $\text{Ra}^{224}$ ,  $\text{Ra}^{226}$ ,  $\text{Th}^{226}$ , and  $\text{Th}^{228}$  (all in the region from 417 to 517 keV).

Thus, the strongest predictions of the model are the existence of low-lying  $\beta$  vibrations ( $\sim 665$  keV) at the beginning of the region of deformation in the rare earths and ( $\sim 450$  keV) at the beginning of the region of deformation in radium and the actinides [see the end of Sec. III.B (5)].

(5) *Reservations Regarding the Constancy and Meaning of  $b$*

The necessity to have a value  $b$  reminds one of the factor 2-5 between moments of inertia calculated from the hydrodynamical model and those observed experimentally. This factor varies with the deformation.<sup>7</sup> Nonetheless, here there is the implicit assumption that the assumed value of  $b$  (2.12) is constant for all values of the deformation and is the same for both  $\beta$  and  $\gamma$  vibrations.

There is no *a priori* reason to expect this constancy, and therefore we must be extremely cautious in accepting it. It will be of value to obtain experimental information on other sets of  $\beta$  and  $\gamma$  vibrational bands (see end of this section). This information will allow a more complete testing of the constancy of  $b$  for both  $\beta$  and  $\gamma$  vibrations and for variations in the deformation. At present there are no contradictions to the assumption of constancy for  $b$ .

Another practical difficulty in using the method is that it is strongly affected by small experimental errors in measurements of the energy of the ground state rotational band. When the  $B$  values are small, even inaccuracies of 0.1 keV in the energy of the first excited state cause a considerable error in the calculation of the vibrational bands. The values of  $b$  from the ground state rotational band in  $\text{Pu}^{238}$  and from the observed  $\beta$  and  $\gamma$  vibrations differ by approximately 10% depending on whether the first excited state is assigned as 44.03 or 44.11 keV.

Several additional pieces of data have become available since these calculations were completed.  $\beta$  vibrations have been found in  $\text{Gd}^{154}$  at 692 keV [Ove Nathan (private communication, January, 1959)] and in  $\text{Sm}^{152}$  at 685 keV [Hultberg and Nathan, Nuclear Phys. (submitted for publication)] in excellent agreement with predictions.

Furthermore, the 4+ state in  $\text{Os}^{188}$  has been determined as 478 keV [R. M. Diamond and J. M. Hollander, Nuclear Phys. **8**, 143 (1958) and P. S. Fisher and R. A. Naumann, Phys. Rev. **112**, 1717 (1958)]. By using the values 155.0 keV and 478 keV, values for  $B$  and  $\hbar^2/\mathcal{J}$  of  $138.11 \times 10^{-3}$  keV and 53.32 keV, respectively, have been determined. By using the value 633 keV for the  $\gamma$  vibration, one calculates the value 1479 keV for the  $\beta$  vibration. 0+ states have been observed in  $\text{Os}^{188}$  at 1086 and 1765 keV (see reference 30). There are indications (see Sec. VII.D) that the 1765 keV is most reasonably classified as the  $n_\gamma=2$ ,  $n_\beta=0$ ,  $K=0$ , two-phonon vibration, whereas the 0+ level at 1086 keV is more nearly the  $\beta$

vibration. Actually, the two vibrations are probably somewhat mixed (see Fig. 10). If this is correct, we should compare an energy somewhere between 1086 and 1765 keV but nearer 1086 keV with the calculated value at 1479 keV. Although this prediction is then not quantitatively verified, the qualitative agreement is gratifying in view of the fact that in  $\text{Os}^{188}$  we are going away from deformed nuclei toward  $\gamma$  unstable nuclei. It is also gratifying that the experimental evidence seems to preclude the possibility of this third vibrational band mixing to any appreciable extent with the ground state band, since it is forbidden by vibrational selection rules (see Sec. VII.D). However, the  $\beta$  vibration calculated for  $\text{Os}^{190}$  seems much too high.  $\text{Os}^{190}$  seems to be a hybrid nucleus with properties intermediate between a deformed nucleus and a gamma unstable nucleus. Therefore, it is not surprising that this hydrodynamical treatment of  $\text{Os}^{190}$  as a normally deformed nucleus fails to predict the  $\beta$  vibration accurately.

Finally,  $\beta$  and  $\gamma$  vibrations have been found recently in  $\text{Th}^{230}$  at 634 and 783 keV, respectively [O. B. Nielsen (private communication, June, 1959)]. In Table III these vibrations were guessed as 754 and 970 keV, respectively. They were therefore predicted high by 120 and 187 keV, respectively. The possibility that these vibrations were high was recognized prior to their discovery and attention drawn to this possibility by the arrow and question mark in Fig. 6. If, instead of using the values of Ong Ping Hok *et al.* (Table III), the values 52.4 and 170 keV are used for the 2+ and 4+ states of  $\text{Th}^{230}$  [reference 14, p. 151; J. O. Rasmussen, Phys. Rev. **113**, 1593 (1959)], the calculated values of  $B$  and  $\hbar^2/\mathcal{J}$  are  $16.67 \times 10^{-3}$  and 18.87 keV, respectively. By using the measured value for the  $\gamma$  vibration, 783 keV, one calculates a value of 581 keV for the  $\beta$  vibration. Thus, the experimental values for the 2+ and 4+ states give calculated values for the vibrations which bracket the experimental values.

As mentioned, it would be somewhat of an accident if the correction factor  $b$  to the hydrodynamical expressions should turn out to be the same for  $\beta$  and  $\gamma$  vibrations and independent of deformation. Furthermore, there may be some other contributions to  $b$  from other types of intrinsic excitation. Indeed, it might seem wisest to define 3 constants for the  $\beta$  and  $\gamma$  vibrations and effects arising from other intrinsic excitations. Some or all of these 3 constants might also be made deformation dependent. Such a treatment must of necessity fit the data better and, perhaps as more and more data become available, such refinements will prove necessary.

#### IV. VIBRATIONAL AND ROTATIONAL LEVEL SYSTEMATICS IN THE RARE EARTHS AND ACTINIDES

The energy of vibration levels above the ground state is plotted as a function of neutron number in Figs. 5-8. Figures 5 and 6 show positive parity levels in the rare

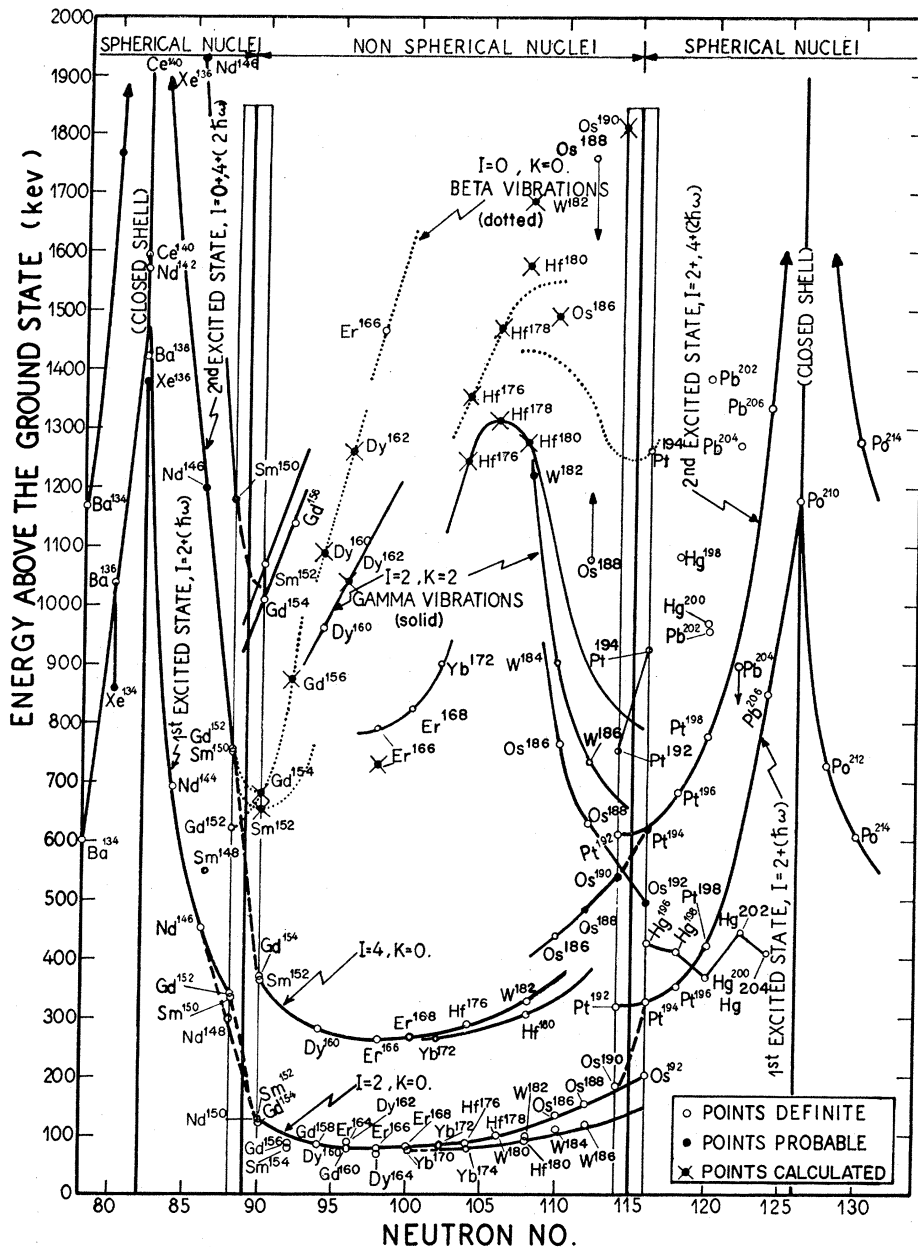


FIG. 5. Positive parity levels of even-even nuclei in the regions between closed neutron shells 82 and 126. Only  $0^+$ ,  $2^+$ , and  $4^+$  members of the ground state bands are plotted; lines connecting the  $\beta$  vibrations are dotted and those connecting the  $\gamma$  vibrations are solid; higher members of the  $\beta$  and  $\gamma$  vibrational bands are not plotted. References: Most of the levels are taken from Strominger, Hollander, and Seaborg, *Revs. Modern Phys.* **30**, 585 (1958) and reference 10. Additional references:  $0^+$ ,  $Gd^{152}$ ; O. Nathan (private communication).  $Gd^{156}$ ; reference 22.  $4^+$ ,  $Os^{188}$ ; P. S. Fisher and R. A. Naumann, *Phys. Rev.* **112**, 1717 (1958).  $2^+$ ,  $W^{184}$  and  $W^{186}$ ; reference 25.  $2^+$ ,  $Er^{166}$ ; references 18 and 19.  $2^+$ ,  $Er^{168}$ ; Jacob, Mihelich, and Handley, *Bull. Am. Phys. Soc. II* **3**, 358 (1958).  $4^+$ ,  $Os^{186}$ ; R. M. Diamond and J. M. Hollander, *Nuclear Phys.* **8**, 143 (1958).  $0^+$ ,  $Os^{188}$ ; Marklund, Van Nooijen, and Grabowski, reported at the Annual Meeting of the Swedish Physical Society (June, 1959), and Nathan, Bes, and Nilsson (private communication). The two  $0^+$  states in  $Os^{188}$  at 1086 and 1765 keV may be mixed (see Sec. VII.D). This would force them apart in energy. This possibility is indicated by arrows which point to the energy region where the states would be if not mixed. The trend in  $\beta$  vibrations (dotted line) is drawn through this region;  $0^+$ ,  $Pt^{194}$ ; I. Marklund, reported at the Annual Meeting of the Swedish Physical Society (June, 1959), and O. Nathan (private communication).

earth and actinide regions, respectively, and Figs. 7 and 8 show negative parity levels. The graphs are divided into vertical sections. In Fig. 5 the central vertical section encloses the deformed nuclei, whereas the two outer vertical sections involve spherical nuclei. In Figs. 6-8, the vertical section on the left encloses spherical nuclei and that on the right deformed nuclei. The heavy vertical lines divide the regions of spherical and deformed nuclei and mark the position of closed shells. The light vertical lines indicate regions of uncertainty where the nucleus may be deformed or spherical. This uncertainty arises from the fact that the deformation is proton as well as neutron dependent.

#### A. Positive Parity Levels of Even-Even Nuclei in the Rare Earths and Actinides

The vibrational and rotational positive parity level systematics of even-even nuclei in the rare earth and actinide regions is shown in Figs. 5 and 6. In the deformed regions, the ground state rotational band is recorded only to the  $4^+$  state (labeled  $I=2, 4$  and  $K=0$ ) to avoid confusion. Furthermore, the band heads of the  $\beta$  and  $\gamma$  vibrational bands (labeled  $\beta$  vibration,  $I=0, K=0$  and  $\gamma$  vibration,  $I=2, K=2$ ) are recorded without any of the superimposed rotational bands which are often experimentally observed. Ex-

perimental levels are light or dark circles depending on whether the data are conclusive in indicating the assignment or are only consistent with it. Calculated levels are indicated with circles with large crosses through them indicating their lack of precision. In the spherical regions, the levels are labeled first and second excited state. Second excited states in the region preceding deformation have been labeled  $I=0+, 4+$ , whereas they have been labeled  $I=2+, 4+$  in the region after deformation. This seems to be in accord with the meager experimental information available. No attempt has been made to present all the data in the spherical region since we are primarily concerned with deformed nuclei.

Solid lines are drawn between vibrational states in the spherical region and between  $\gamma$  vibrational states and rotational states in the deformed region. Dotted lines are drawn between  $\beta$  vibrational states.

The difficulty of presenting both the proton and neutron dependence in two dimensions is obvious. We have chosen a plot against neutron number and may think of the diagrams as a superposition of a series of true two-dimension diagrams in which the proton number is held constant. Then the separate diagrams for single proton numbers become contour lines in the proton dependence. This situation is especially clear in the region from neutron number 100 to 114. The contour lines for the  $2+$  and  $4+$  rotational states and for the  $2+$  gamma vibrational state for various  $Z$  define three surfaces.

Particularly significant in Figs. 5 and 6 are the smooth trends for the vibrations. This seems to argue strongly for their identification as vibrations with small enough admixtures of other states so that their systematics remain intact. A second interesting feature is the smooth way in which the vibrations of the spherical nuclei join the vibrations of the deformed nuclei. This joining is especially smooth in the region from neutron number 110 to neutron number 120. There the  $4+$  state of ground state rotational band and the  $2+$   $\gamma$  vibrational band head join very smoothly onto the second vibrational state of the spherical region.

The trends of the vibrations in the deformed regions themselves are also of importance. The  $\beta$  vibrations both at the beginning of the region of deformation in the rare earths and the actinides are relatively near the ground state but seem to go monotonically upward as one goes through the region of deformation tending downward only at the end of the region of deformation. The  $\gamma$  vibrations seem to be more complex, oscillating rather wildly at the beginning of the region of deformation, then going through a minimum and then a maximum in the region of  $W^{182}$ . The trend thereafter is drastically down but very smooth in joining the second vibrational state of the spherical region. Much of the information on trends may be summarized by saying that *the nucleus is particularly "soft" to positive parity vibrations in regions where it changes from spherical to deformed or from deformed to spherical.*

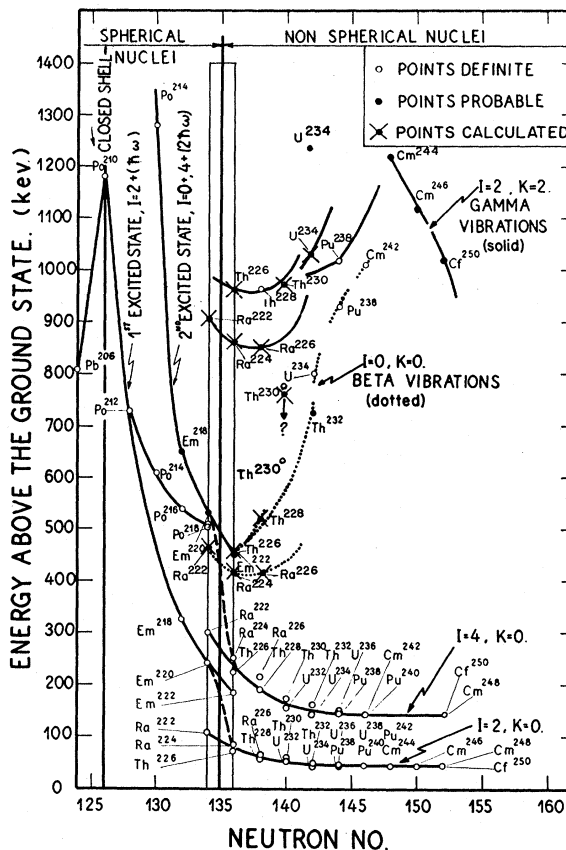


FIG. 6. Positive parity levels of even-even nuclei in the region above neutron number 126. Only  $0+$ ,  $2+$ , and  $4+$  members of the ground state bands are plotted; lines connecting the  $\beta$  vibrations are dotted and those connecting the  $\gamma$  vibrations are solid; higher members of the  $\beta$  and  $\gamma$  vibrational bands are not plotted. References: The levels are taken from Strominger, Hollander, and Seaborg, *Revs. Modern Phys.* **30**, 585 (1958) and reference 10.  $Cm^{244}$ ,  $Cm^{246}$ , and  $Cf^{250}$ ; B. R. Mottelson (private communication).  $0+$ ,  $2+$ ,  $Th^{230}$ ; O. B. Nielsen (private communication).  $2+$ ,  $U^{234}$ ; C. J. Gallagher and T. D. Thomas, *Bull. Am. Phys. Soc.* **II** **4**, 293 (1959).

## B. Negative Parity Levels of Even-Even Nuclei

In the deformed nuclei the lowest-lying negative parity vibrations ( $\lambda=3$  and  $\nu=0, \pm 1, \pm 2$ , and  $\pm 3$ ) should be octupole vibrations. The systematics of one set of these vibrations with  $K=0$  and  $I=1-, 3-, 5-$ , etc. has been previously studied.<sup>20</sup> On the other hand, in the spherical region the lowest-lying octupole vibration should have  $I=3-$ . The systematics of these vibrations are presented in Figs. 7 and 8. The same conventions have been used as for the positive parity levels. No discussion of the nuclear surface is warranted in view of the sparsity of data.

There is some evidence for the systematic occurrence of a  $2-$  band, presumably with  $K=2$ . While this suggests that the band is collective in nature, the suggestion must be considered tentative until more data

<sup>20</sup> Stephens, Asaro, and Perlman, *Phys. Rev.* **96**, 1568 (1954); **100**, 1543 (1955).

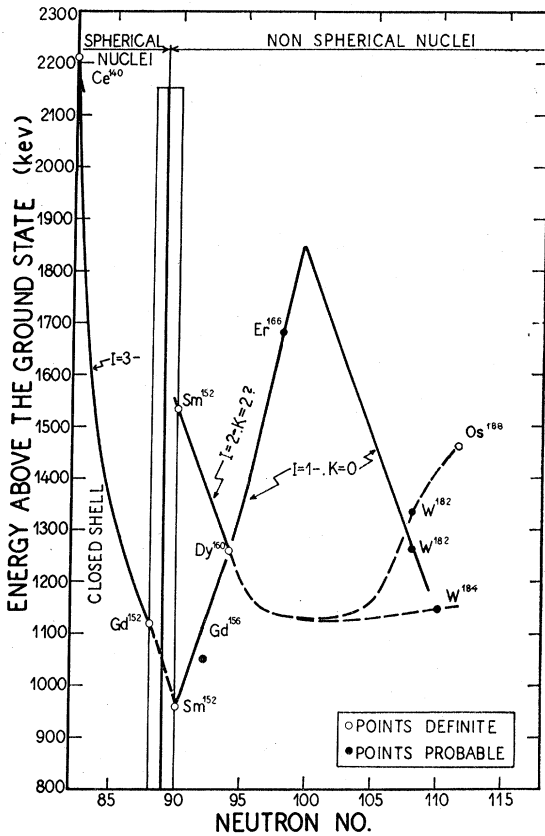


Fig. 7. Negative parity levels of even-even nuclei above neutron number 82. Only band head states are plotted. References: Most of the levels are taken from Strominger, Hollander, and Seaborg, *Revs. Modern Phys.* **30**, 585 (1958). Additional references:  $Gd^{166}$  ( $1-$  guessed from probable  $3-$ ); reference 22.  $W^{184}$ ; Gallagher, Strominger, and Unik, *Phys. Rev.* **110**, 725 (1958).  $2-$ ,  $Os^{188}$ ; Marklund, Van Nooijen, and Grabowski, reported at the Annual Meeting of the Swedish Physical Society (June, 1959), and Nathan, Bes, and Nilsson (private communication).

are available. Of particular interest is the fact that the  $3-$  state of  $Gd^{152}$  (a spherical nucleus) lies in the vicinity of the  $1-$  octupole rotational band in the deformed nucleus  $Sm^{152}$ , thereby suggesting their relatedness. It is also of interest to note that although the  $3-$  (spherical)  $1-$  (deformed) octupole vibration lies especially low in the regions of shifting over from a spherical to a deformed nucleus, the opposite is true of the systematically occurring  $2-$  level.

The  $K=0$ ,  $I=1-, 3-, 5-$ , etc. bands are of particular interest to the theorists. In the first place, their branching ratios to the ground state rotational band indicate greater purity of the states than is found for the  $\beta$  and  $\gamma$  vibrational bands. Secondly, their moments of inertia seem to be more uniform relative to the ground state. Finally, they may afford an answer to the question, "Is there a permanent octupole type of deformation in nuclei?" If the octupole vibration is not permanent as seems most reasonable, one may hope to observe a higher  $0+, 2+, 4+$ , etc. band approximately

double the energy of the first octupole vibrational band above the ground state, decaying by  $E1$  preferentially to the  $I=1-, 3-, 5-, K=0$  states rather than to the ground state rotational band.

## V. INTERPRETATION OF THE POSITIVE PARITY LEVEL SYSTEMATICS

After having looked in an empirical way at the systematics of positive parity levels in Figs. 5 and 6, it is then worthwhile to see if the additional information we gain about vibrations in deformed nuclei can add to our information about and aid our understanding of the vibrations of spherical nuclei.

### A. Relationships between Positive Parity Levels in Deformed and Spherical Nuclei

The empirical information has already been summarized in Sec. IV. We shall be considering spherical, " $\beta$  unstable," normally deformed, and  $\gamma$  unstable nuclei. Since, in some sense, all of these nuclei have the same degrees of freedom, *viz.*,  $\alpha_\mu$  for the spherical nuclei

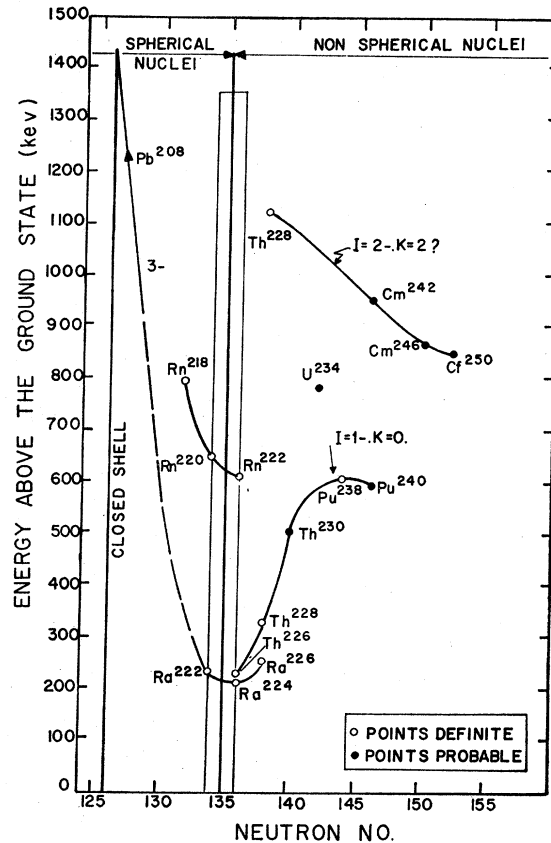


Fig. 8. Negative parity levels in even-even nuclei above neutron number 126. Only band head states are plotted. References: Most of the levels are taken from Strominger, Hollander, and Seaborg, *Revs. Modern Phys.* **30**, 585 (1958).  $Cm^{242}$ ,  $Cm^{246}$ , and  $Cf^{250}$  from B. R. Mottelson (private communication).  $2-$ ,  $Th^{228}$ ; S. Bjornholm (private communication).  $1-$ ,  $U^{234}$ ; C. J. Gallagher and T. D. Thomas, *Bull. Am. Phys. Soc.* **II** 4, 293 (1959).

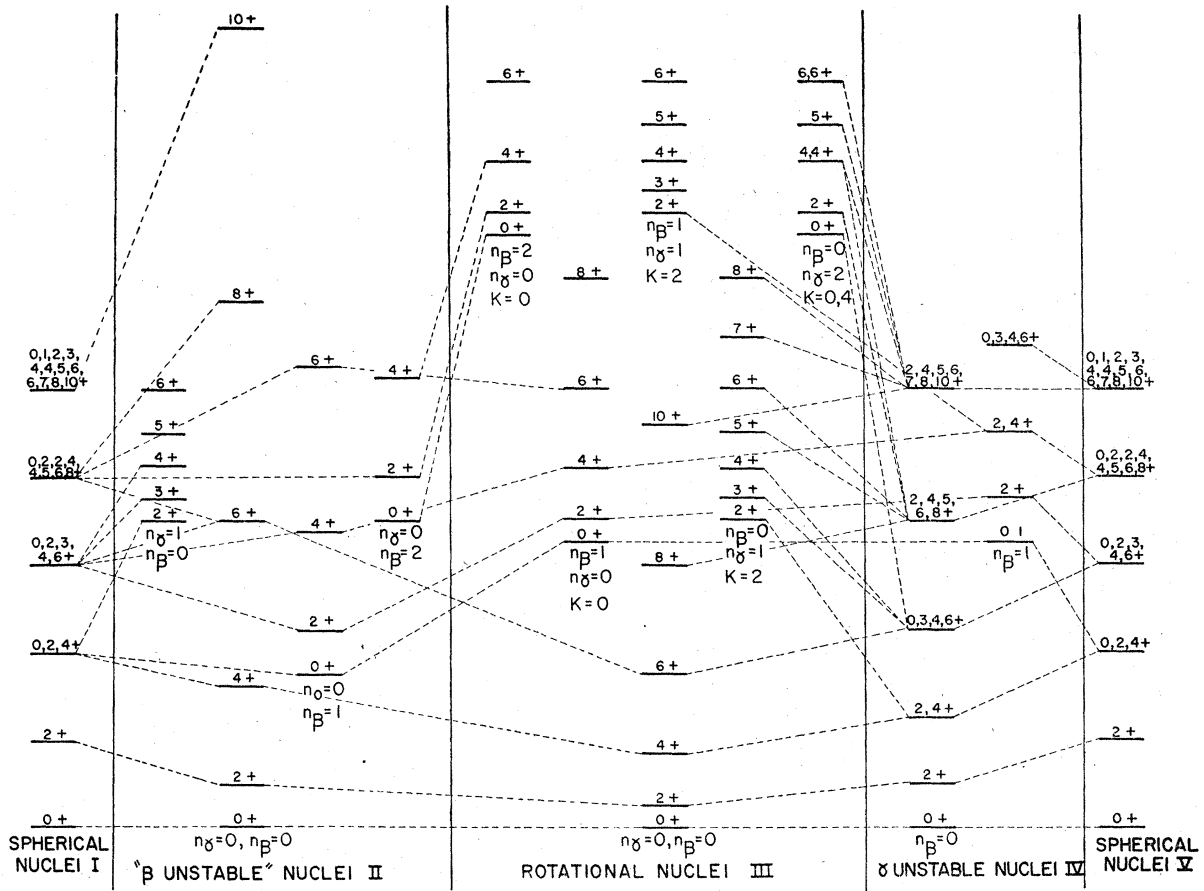


FIG. 9. Relationships between the levels in spherical, deformed, "β unstable," and γ unstable nuclei. Vertical solid lines separate the various nuclear species. Spins are given on top of the levels. Related states are connected by dashed lines.

and  $\beta$ ,  $\gamma$ ,  $\theta_i$  for the normally deformed nuclei (each having five coordinates), there must be a definite relationship between each of the types of spectra.

(1) *The Graph*

Figure 9 presents a schematic representation of relationships between spherical and deformed nuclei by using intermediate regions involving "β unstable" nuclei and γ unstable nuclei. The different types of nuclear levels are set apart by vertical lines and labeled I, II, III, IV, and V. I and V are the same and therefore the sequence I through V represents a transition from one approximately closed-shell region to another. The relationship between states is shown by connecting the related states with dashed lines. To avoid confusion, many of the higher energy states are not connected. A "β unstable" vibration must involve an infinitely long nucleus. Since there is no physical meaning to such a nucleus, the term "β unstable" is put in quotations and Fig. 9 presents the level scheme as that of a deformed nucleus in which the β vibration lies unusually close to the ground state and recurs at low energy intervals. A number of idealizing assumptions were necessary in

order to construct Fig. 9. They are listed without further comment:

(i) Arbitrarily, the ratio of first excited states in (a) spherical nuclei, (b) "β unstable" and γ unstable nuclei, and (c) deformed nuclei is 4:2:1.

(ii) The ratio of excited states for a spherical nucleus is 1:2:3:4:5, for a "β unstable" and deformed nucleus is 1:3.33:7.0:12, and for a γ unstable nucleus is 1:2.5:4.5:7:10.

(iii) The γ and β vibrations in the deformed region, the vibration in the "β unstable" region, and the β vibration in the γ unstable region are assumed to lie at the same place (at approximately 14 times the first excited state in deformed nuclei and 7 times the first excited state in "β unstable" and γ unstable nuclei).

(iv) With the exception of the "β unstable" nuclei, strict adherence to simple models with complete degeneracies is maintained.

(2) *Energy Relationships between the 0+, 2+, and 4+ Members of the Vibrational Bands of Spherical Nuclei*

Ideally, the second excited state of a spherical nucleus is a degenerate triplet with spins 0+, 2+, and 4+.

Experimentally, this degeneracy is usually broken and varying orders of the various members of the triplet are seen. Table IV lists the second excited state multiplets of a number of even-even nuclei. Nuclei at the beginning and at the end of the  $A=150-190$  region of deformation are included in the table for comparison with their neighboring undeformed even-even nuclei. By using Table IV in conjunction with Fig. 9, an interesting relationship emerges. Nuclei which are close to the beginning of the region of deformation have their  $0+$  and  $4+$  states close together and the  $2+$  state, if observed, lies at considerably higher energies. At the end of the region of deformation, the  $2+$  and  $4+$  states lie close together and the  $0+$ , if observed, considerably higher. This is clearly predicted in Fig. 9. Thus, in the regions between I and II, the  $0+$  and  $4+$  lie low and the  $2+$  high and in the region around IV in Fig. 9, the  $2+$  and  $4+$  lie low and  $0+$  high. This would lead one to predict that this is a general tendency to be expected in nuclei preceding and following the regions of deformation.

TABLE IV. Second excited state multiplets of certain even-even nuclei.

Nucleus	Second excited state multiplets. Ratio of energy of state to energy of ground state; spin given in parentheses		
	Lowest member	Next member	Highest member
$^{106}_{46}\text{Pd}$	2.18 (2+)	2.21 (0+)	
$^{108}_{46}\text{Pd}$	2.20 (2+)	2.41 (0+)	
$^{110}_{48}\text{Cd}$	2.10 (2+)	2.16 (?)	2.35 ((4+))
$^{114}_{48}\text{Cd}$	2.18 (2+)	2.31 (4+)	2.35 (0+)
$^{152}_{64}\text{Gd}$	1.79 (0+) <sup>a</sup>	2.20 (2+ or 4+)	
$^{152}_{62}\text{Sm}$	3.01 (4+)	5.62 (0+) <sup>a</sup>	8.88 (2+)
$^{164}_{64}\text{Gd}$	3.01 (4+)	5.51 (0+) <sup>a</sup>	8.11 (2+)
$^{188}_{76}\text{Os}$	3.09 (4+)	4.08 (2+)	7.01 (0+) <sup>b</sup> 11.39 (0+) <sup>b</sup>
$^{190}_{76}\text{Os}$	2.92 (4+)	2.96 (2+)	
$^{192}_{78}\text{Pt}$	1.93 (2+)	2.48 ((4+))	(3.66 (0+)) <sup>b</sup>

<sup>a</sup> Ove Nathan (private communication) (to be published).

<sup>b</sup> Marklund, Van Nooijen, and Grabowski, reported at the Annual Meeting of the Swedish Physical Society (June, 1959); Nathan, Nilsson, and Bes (private communication). These states may have considerable  $n_\gamma = 2$ ,  $n_\beta = 0$  character (see e.g., Figs. 9 and 10).

One might further speculate that when a near-lying triplet occurs as in the case of  $\text{Cd}^{114}$  (and possibly  $\text{Pd}^{106}$ ,  $\text{Pd}^{108}$ , and  $\text{Cd}^{110}$ ), this happens as a consequence of the fact that the neutron number is similar to that at the beginning of the region of deformation whereas the proton number is similar to that at the end of a region of deformation.

To generalize these ideas, we suggest that when the neutron and proton shells are out of phase (one shell is being completed as the other is just beginning), moderately close-lying triplets are expected. When the neutron and proton shells are in phase, closely lying  $0+$  and  $4+$  states and higher-lying  $2+$  states are to be expected following approximately double-shell closure, and closely low-lying  $2+$  and  $4+$  states and higher-lying  $0+$  states are to be expected near the next approximate double-closed shells.

TABLE V. Construction of the  $\gamma$  unstable vibrational band from the bands of a normal deformed even-even nucleus.

State	Spins of degenerate levels participating in the state						
	12	9, 10	6	7, 8	3, 4	0	6
6th	10	7, 8	4	5, 6	2		
5th	8	5, 6	2	4			
4th	6	3, 4	0				
3rd	4	2					
2nd	2						
1st	0						
G.S.	0						
$K$	0	2	0	4	2	0	6
	$K$ quantum number in the related deformed nucleus						
$n_\gamma$	0	1	2	2	3	3	3
$n_\beta$	0	0	0	0	0	0	0
	$n_\gamma$ and $n_\beta$ quantum numbers of the rotational bands of the related deformed nucleus						

### (3) Procedure for Constructing " $\beta$ Unstable," $\gamma$ Unstable, and Spherical Nuclear Level Systematics from the Rotational Bands of Deformed Nuclei

The complexity of Fig. 9 is obvious in spite of the fact that the systematics is not carried very far. Therefore, it is important to develop a formal method of showing the relationship between deformed nuclei and other nuclei. This is done by making arrays of numbers in which each number or series of horizontal numbers represents a level in that particular nucleus.

(i) The procedure of constructing  $\gamma$  unstable and spherical nuclear level systematics from the rotational bands of deformed nuclei.—Table V shows how the lowest  $\gamma$  unstable vibrational band is constructed from the rotational bands of a deformed nucleus. All horizontal numbers represent levels in a  $\gamma$  unstable nucleus. The lowest three horizontal columns show the relationship between the deformed nucleus and the lowest  $\gamma$  unstable vibrational band.

Table VI shows the construction of a spherical nuclear vibrational band from a series of identical  $\gamma$  unstable bands and the relationship to both the deformed nuclear bands and the  $\gamma$  unstable bands.

(ii) The procedure of constructing " $\beta$  unstable" and spherical nuclear level systematics from the rotational

TABLE VI. Construction of the vibrational bands of spherical even-even nuclei from a series of  $\gamma$  unstable vibrational bands.

State	Spins of degenerate levels participating in the state			
	0, 3, 4, 6, 6, 7, 8, 9, 10, 12	2, 4, 5, 6, 8	2, 4	0
6th	2, 4, 5, 6, 7, 8, 10	0, 3, 4, 6	2	
5th	2, 4, 5, 6, 8	2, 4	0	
4th	0, 3, 4, 6	2		
3rd	2, 4	0		
2nd	2			
1st	0			
G.S.	0			
$n_\beta$	0	1	2	3
	$n_\beta$ quantum number of the vibrational bands of the related $\gamma$ unstable nucleus			
$n_\gamma$	0, 1, 2, 3	0, 1, 2	0, 1	0
$n_\beta$	0	1	2	3
	$n_\gamma$ and $n_\beta$ quantum numbers of the rotational bands of the related deformed nucleus			

bands of deformed nuclei.—Table VII presents first, a sequence of “ $\beta$  unstable” vibrational bands which when used as building blocks can be used to construct the spherical nuclear vibrations. Although the  $\gamma$  unstable bands are all identical, the “ $\beta$  unstable” bands are not. It is physically untenable to consider a true “ $\beta$  unstable” nucleus, but it is possible to construct the levels formally as shown in Table VII. The lowest three horizontal columns point out the relationships between spherical and “ $\beta$  unstable” vibrational bands and the vibrational and rotational bands of a deformed nucleus.

Nuclei in the regions of neutron number  $\sim 90$  and  $\sim 114$  are in the transition region between deformed and spherical regions (see Fig. 5). Consequently, a large coefficient ( $B$ ) in the  $I^2(I+1)^2$  correction term must be applied to attempt to correct the energy level sequences to simple  $I(I+1)$  dependences (see Table II). Although this correction works nicely for  $\text{Sm}^{152}$  and  $\text{Gd}^{154}$ , it does not work nearly so well for  $\text{Os}^{190}$ . This difference may be related to the fact that there is no physical meaning to

TABLE VII. Construction of the vibrational bands of spherical even-even nuclei from a series of  $\beta$  unstable vibrational bands.

State	Spins of degenerate levels participating in the state													
6th	12	8	4	0	9, 10	5, 6	2	6	7, 8	2	4	3, 4	0	6
5th	10	6	2	7, 8	3, 4		4	5, 6	0		2			
4th	8	4	0	5, 6	2		2	4						
3rd	6	2		3, 4			0							
2nd	4	0		2										
1st	2													
G.S.	0													
$n_\gamma$	0			1			2			3				
	$n_\gamma$ quantum number of the vibrational bands of the related $\beta$ unstable nucleus													
$n_\beta$	0	1	2	3	0	1	2	0	0	1	1	0	0	0
$n_\gamma$	0	0	0	0	1	1	1	2	2	2	2	3	3	3
	$n_\gamma$ and $n_\beta$ quantum numbers of the vibrational bands of the related deformed nucleus													

a “ $\beta$  unstable” nucleus and as one approaches “ $\beta$  instability,” the geometrical shape of the nucleus is that of an ordinary deformed nucleus with the consequent  $I(I+1)$  energy dependence of a deformed nucleus. On the other hand, the nucleus which is approaching the  $\gamma$  unstable type is approaching a physically reasonable nuclear type which has a different  $I$ -energy dependence.<sup>21</sup>

As one approaches the “ $\beta$  unstable” region from the spherical region [in the rare earths as one approaches the region of 90-neutron nuclei ( $\text{Sm}^{152}$ — $\text{Gd}^{152}$ ) from lower neutron number], there is a discontinuity in the level systematics; but as one continues through the region of deformation, the change into spherical nuclei at  $\sim \text{Pb}^{206}$  does not result in a similar discontinuity in the vicinity of  $\text{Os}^{190}$  (see e.g., Fig. 5). This difference in level systematics may possibly be explained by the fact that at  $\text{Os}^{190}$  one is approaching a physically meaningful  $\gamma$  unstable nucleus which is intermediate between a

deformed and a spherical nucleus, but at  $\text{Sm}^{152}$ — $\text{Gd}^{152}$  there is no corresponding intermediate situation with physical meaning.

#### (4) Problem of Crossing of Levels with the Same Spin and Parity

In Figs. 5 and 6 the systematics of nuclear levels in the deformed region indicate that the position of  $\beta$  and  $\gamma$  vibrational bands varies considerably from the beginning of the region of deformation to the end in such a way that these bands tend to cross. Since members of each of the bands have certain spins and parities in common, these states should perturb each other with associated mixing or hybridization.

Little is known experimentally about the degree of mixing of these states. If  $K$  were an extremely good quantum number, one would expect very little mixing of the states and a simple crossover. This is true because bands which differ in  $K$  by 2 or more, or do not differ at all in  $K$ , could not mix if  $K$  were a good quantum number. However, we have evidence of many kinds that  $K$  is not an extremely good quantum number and that, for example, the ground state rotational band is mixed with the  $\gamma$  vibrational band through the medium of a common amount of mixture of a  $K=1$  band of considerably higher energy (see Sec. VII).

Since we have experimental evidence for the mixing of the ground state  $K=0$  and the  $\gamma$  rotational band  $K=2$ , we can be virtually certain that the  $\beta$  vibrational

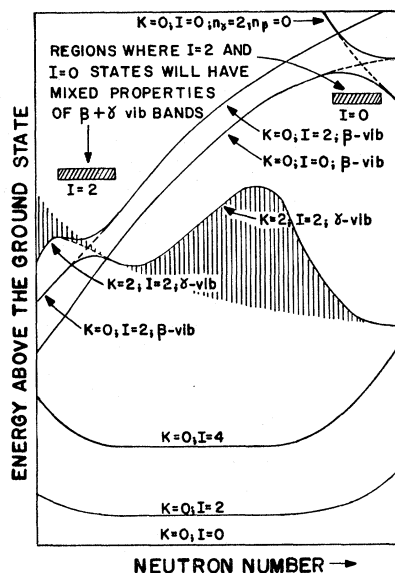


Fig. 10. Schematic diagram of the levels in the region  $A \sim 150$ — $190$  showing the mixing of the  $K=2$ ,  $I=2$ ,  $\gamma$  vibration and the  $K=0$ ,  $I=2$ ,  $\beta$  vibration, and the possible mixing of the two-phonon  $n_\gamma=2$ ,  $n_\beta=0$  band and the  $n_\gamma=0$ ,  $n_\beta=1$  normal  $\beta$  band. The slanted hatched rectangular area is the region in which mixing of the levels occurs. The vertical hatched area corresponds to deviations in the general trend of the  $\gamma$  vibrations due to the presence of levels from other shells.

<sup>21</sup> L. Willets and M. Jean, Phys. Rev. **102**, 788 (1956).

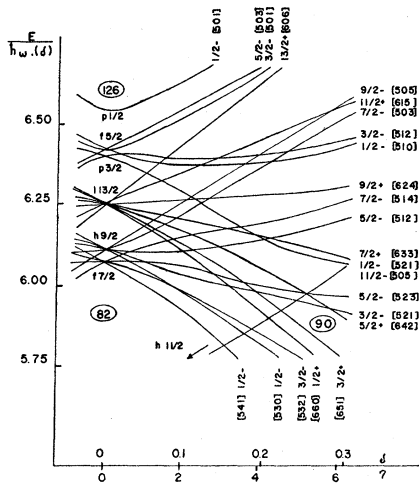


FIG. 11. Single-particle levels for odd  $N$  nuclei in the region  $82 < N < 126$ . The asymptotic quantum numbers  $[N n_z A]$  are listed in brackets (reference 22).

band ( $K=0$ ) will mix with the  $\gamma$  vibrational band ( $K=2$ ).

Furthermore, it seems probable that the  $n_\gamma=2, n_\beta=0, K=0$  band will mix to some extent with the  $n_\gamma=0, n_\beta=1, K=0$  band even though this mixing is vibrationally forbidden (see Sec. VII.D). In this latter case the experimental data do not tell whether or not actual crossings occur, although it is assumed in Fig. 10. A schematic representation of these phenomena is shown in Fig. 10 together with an indication of the regions of deformation in which they are expected. This situation is well known in molecular spectroscopy. [See e.g., G. Herzberg, *Spectra of Diatomic Molecules* (D. Van Nostrand Company, Inc., Princeton, New Jersey, 1950), p. 282.] The shift of a given state depends inversely on its separation in energy from another state of the same spin and parity. The smaller the separation of the two states, the larger are their shifts. The higher energy state is displaced upward, and the lower energy state is displaced an equal amount downward. Each of the two states assumes some of the properties of the other state, producing a kind of hybrid. In Fig. 10 this hybrid is shown for the  $K=2, I=2, \gamma$  vibrational band state and the  $K=0, I=2, \beta$  vibrational state. For simplicity, this type of interaction for the other states of the  $\beta$  and  $\gamma$  vibrational bands which have a common spin and parity have not been shown in Fig. 10. All members of the  $\beta$  vibrational band except the  $I=0$  state and all members of the  $\gamma$  vibrational state except those states which have odd spin can be expected to mix in a similar way. Similar statements apply to the mixing of the  $n_\gamma=2, n_\beta=0, K=0$  and the  $n_\gamma=0, n_\beta=1, K=0$  bands. However, in this case each state in the bands should mix. Thus, whereas there is some energy ambiguity caused in the  $\gamma$  band by mixing between it and the  $\beta$  band at the beginning of the region of deformation, a similar ambiguity may be caused at the end of the

region of deformation by the mixing of the  $0+$   $\beta$  band head state and the two-phonon gamma band. The  $n_\gamma=2, n_\beta=0, K=4$  band may also mix especially with the higher members of the  $\gamma$  vibrational band, but also with the  $\beta$  vibrational band. The exact extent of the region in which this mixing should occur, indicated in Fig. 10 by cross-hatched areas, is not defined at present by experiment.

## B. Systematics of $\beta$ and $\gamma$ Vibrations

Figure 10 also attempts to indicate schematically the trends of  $\beta$  and  $\gamma$  vibrations when plotted against neutron number for deformed nuclei in the rare earth region between closed shells of 82 and 126 neutrons. There seems to be a strong indication that  $\beta$  vibrations at the beginning of the region of deformation have very low energy. The information on the rest of the region of deformation is scanty. It involves largely calculated values of  $\beta$  vibrational bands. What little information is available seems to indicate that  $\beta$  vibrations increase more or less continuously across most of the region of deformation, reaching their maximum value near the end of this region and then decreasing as the transition from deformed to spherical nuclei is made. Conversely,  $\gamma$  vibrations might be thought of as decreasing as one goes from the beginning of a region of deformation across the region of deformation. Superimposed on this gross structure there is a fine structure—a region from neutron number  $\sim 90$  to neutron number  $\sim 94$  where the  $\gamma$  vibrations lie below this trend and a broad region from neutron number  $\sim 98$  to neutron number  $\sim 108$  in which the  $\gamma$  vibrations seem to lie considerably above the general trend. Such generalized statements need to be qualified by indicating the difficulties which have not been completely overcome in attempting to systematize this kind of experimental data. First, there is both a proton and neutron dependence but so few data that it has been necessary to superimpose the data into a kind of contour map in which the proton number is the hidden variable. Secondly, there are the experimental uncertainties in assigning some of the levels as vibrational bands and the uncertainties in calculation of these bands. Thirdly, there is the presence of fairly wildly oscillating  $\gamma$  vibrational energies at the very beginning of the region of deformation. This may very well be explained by the presence in this region of near-lying  $\beta$  vibrations and the consequent disturbing of the normal position of the  $\gamma$  vibrations. Finally, the information available for  $\beta$  vibrations is considerably less than that for  $\gamma$  vibrations and the smooth trend, without the details observed in the  $\gamma$  vibrations, may really be the result of less complete information.

### (1) Attempt to Explain the Trend in $\gamma$ Vibrations

Figure 11 is taken from a recent article by Mottelson and Nilsson.<sup>22</sup> The deformation for prolate nuclei (only)

<sup>22</sup> B. R. Mottelson and S. G. Nilsson, *Mat. Fys. Skr. Dan. Vid. Selsk. I*, No. 8 (1959).

is indicated on the abscissa, and the energies of the states, together with the spectroscopic description of these states, is given on the ordinate. The degeneracy of the typical shell-model states (at 0 deformation) is partially broken with increasing permanent deformation. At high deformation the levels can be described by a new spectroscopic notation (the asymptotic quantum numbers). They are indicated in brackets in Fig. 11 as  $[Nn_z\Lambda]$ .  $N$ , the first number in the brackets, is the principal quantum number and corresponds to the total number of nodes in the wave function. It is determined by the oscillator shell of the anisotropic harmonic oscillator and its evenness or oddness determines the parity of the state.  $n_z$  is the number of nodal planes perpendicular to the symmetry axis, and  $\Lambda$  is the component of orbital angular momentum along the symmetry axis. It is convenient to define an additional quantum number,  $n_1$ , which is already uniquely determined as  $N - n_z$ . It is the number of nodal planes perpendicular to the other two equivalent minor axes.

Figure 11 therefore gives a diagram of the single particle states for nuclei with odd neutron numbers between 82 and 26. This corresponds to the actual neutron numbers in deformed rare earth nuclei. The levels form a complex network. However, several important trends in the  $n_1$  quantum number demand additional attention. (1) In general, the  $n_1$  quantum number goes from low values to increasingly high values as one goes from neutron number  $N=82$  to  $N=126$ . There are two exceptions, however. (2) In the beginning of the region of deformation among levels of low  $n_1$ , there occurs a level from a lower shell with a very high  $n_1$ . This is an  $11/2^-$  level resulting from the  $h_{11/2}$  shell. The breaking up of this shell has been shown by Mottelson and Nilsson<sup>6</sup> to be responsible for the dramatic increase in deformation in going from neutron number  $N=88$  to  $N=90$ . (3) The spin orbit splitting brings an  $i_{13/2}$  series of levels down into this region of deformation from the shell above. The  $i_{13/2}$  levels bring into the middle of the region of deformation many levels with  $n_1$  particularly low.

It would seem reasonable to explain (1) the general decrease in  $\gamma$  vibrational energy as due to the tendency of the  $n_1$  quantum number to increase as one goes across the shell, (2) the presence of abnormally low  $\gamma$  vibrational energies at the beginning of a region of deformation as due to abnormally high  $n_1$  quantum numbers resulting from the presence of the  $h_{11/2}$  state from the lower shell, and (3) the presence of a broad region of abnormally high  $\gamma$  vibrational energies to a region of abnormally low  $n_1$  quantum numbers as due to the  $i_{13/2}$  levels in this region of deformation because of spin-orbit splitting.

#### (2) Attempt to Explain the Trend in $\beta$ Vibrations

Although one might expect the  $\gamma$  vibrations to be related to the  $n_1$  quantum number, the  $\beta$  vibrations are

|| The author is indebted to D. Bes for illuminating comments on this section.

not related in such a simple way to the  $n_z$  quantum number. Mottelson and Nilsson<sup>22</sup> have shown that there are two minima in the expression for the energy as a function of  $\beta$  for nucleon number 89. This double minimum is really an approximation of a much broader potential curve in  $\beta$  with a consequent considerable lowering of the  $\beta$  vibration in the region of Nd<sup>160</sup>, Sm<sup>162</sup>, and Gd<sup>164</sup>, and in the region of the Ra and Th isotopes. The experimental and calculated information on the  $\beta$  vibrations for these nuclei indicate that they are much lower in energy than the usual  $\beta$  vibration. It is obvious, however, that trends in  $\beta$  vibrations require serious study both by the experimentalist and by the theorist.

## VI. POTENTIAL ENERGY SURFACES

One should be able to calculate the shape of the potentials for  $\beta$  and  $\gamma$  vibrations as the sum of individual particle energies for the  $\beta$  and  $\gamma$  deformation parameters, respectively. Such a calculation should show, for example, that the presence of many near-lying states with high  $n_1$  will broaden the potential curve in the  $\gamma$  coordinate and therefore lower the  $\gamma$  vibrational energy. This calculation is, however, not within the scope of this article. We must content ourselves with schematic diagrams which, while they have no quantitative significance, attempt to mirror schematically the experimental situation. For this purpose we use contour maps in polar coordinates [see, e.g., D. L. Hill and J. A. Wheeler, Phys. Rev. **89**, 1102 (1953)].

### A. Cases of $\gamma$ and $\beta$ Instability

In all of these potential energy plots, contour maps in polar coordinates are used. Thus, lines on the graph correspond to positions of equipotential energy. The  $r$  variable corresponds to the deformation parameter  $\beta$ , whereas the  $\theta$  variable corresponds to the deformation parameter  $\gamma$ .

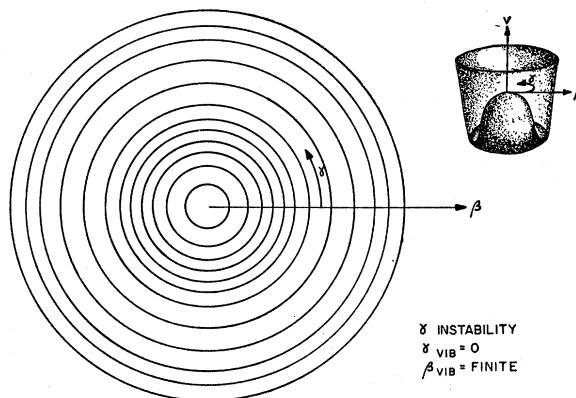


FIG. 12. Contour map of the potential energy diagram for a  $\gamma$  unstable nucleus in polar coordinates. The  $r$  coordinate is the  $\beta$  deformation and the  $\theta$  coordinate is the  $\gamma$  deformation. The inset shows the potential energy diagram in three dimensions.

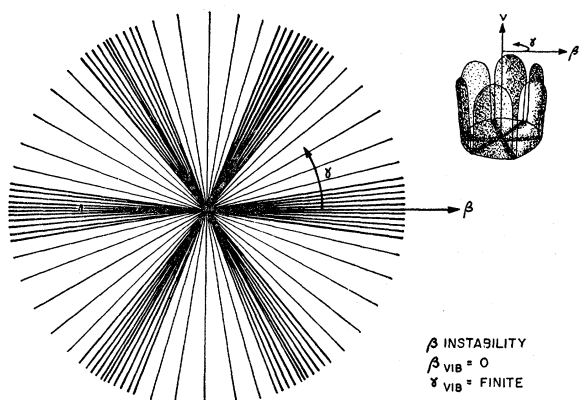


FIG. 13. Contour map of the potential energy diagram for a "beta unstable" nucleus in polar coordinates. The  $r$  coordinate is the  $\beta$  deformation and the  $\theta$  coordinate is the  $\gamma$  deformation. The inset shows the potential energy diagram in three dimensions.

### (1) $\gamma$ Unstable Potential

As first pointed out by Hill and Wheeler, in the case of  $\gamma$  instability it is energetically most feasible to go from prolate to oblate deformations without going through a spherical nucleus. The potential energy surface shown in Fig. 12 illustrates this situation. The inset in Fig. 12 attempts to picture the potential energy surface in three dimensions represented by the contour map. There are no minima or maxima for  $\gamma$  deformations, but there are well-defined minima for  $\beta$  deformations. Whereas the case of  $\gamma$  instability represents an idealization, it is nonetheless a physically tenable one. It seems probable that nuclei like  $\text{Os}^{190}$  and  $\text{Os}^{192}$  may actually approach the condition of  $\gamma$  instability.

### (2) Case of "beta Instability"

Whereas  $\gamma$  instability is physically tenable, "beta instability" is not. Figure 13 is the potential energy diagram for a "beta unstable" nucleus. Since there is no potential minimum and no maximum for a  $\beta$  deformation, a "beta unstable" nucleus would elongate indefinitely and would therefore not be stable. A process similar in many respects to fission should result. For this reason it might be worthwhile to study the fission of those nuclei which approach most closely to "beta instability." These nuclei are the rare earths,  $\text{Nd}^{150}$ ,  $\text{Sm}^{152}$ , and  $\text{Gd}^{154}$ , and  $\text{Ra}^{222}$ ,  $\text{Ra}^{224}$ ,  $\text{Ra}^{226}$ ,  $\text{Th}^{226}$ , and  $\text{Th}^{228}$ . One is led to ask, "Is the unusual fission of  $\text{Ra}^{226}$  due in part to the low-lying  $\beta$  vibration?"

## B. Actual Experimental Situation

Whereas the "beta unstable" and the  $\gamma$  unstable situations represent the extremes, probably all experimental situations lie somewhere in between. Thus, for example, the type of potential energy curve to be expected at the beginning of the region of deformation is shown in Fig. 14.  $\beta$  vibrations lie considerably lower than the  $\gamma$

vibrations. Hence, the potential energy curve in the  $\beta$  coordinate at the prolate minimum has less curvature in the  $\beta$  coordinate than in the  $\gamma$  coordinate. Assumptions have been made about the relative depths of the prolate and oblate minima, but since these potential energy surfaces are schematic, it is important only to indicate that in all cases the prolate minima have been assumed lower than the oblate minima. This is in accord with experimental data.

Figures 15 and 16, respectively, show the potential energy surfaces for nuclei in approximately the middle of the region of deformation, and for nuclei at the end of the region of deformation. Figure 15 assumes that  $\beta$  and  $\gamma$  vibrational energies are approximately the same. This is the case, for example, for  $\text{Pu}^{238}$  (see Fig. 3). In each of the potential energy surfaces the potential at  $\beta=0$  is expected to be flat. In Fig. 16, representing the situation toward the end of the region of deformation, we are approaching  $\gamma$  instability with the  $\gamma$  vibrational energy considerably less than the  $\beta$  vibrational energy. Prolate axial symmetry is favored, but one is approaching  $\gamma$  instability where there is no meaning to prolate and oblate nuclei. The valley, in this case, has local minima and maxima, but the change in potential in growing from prolate to oblate shape is much smaller by following the valley of  $\gamma$  instability than by going over the flat mountain of spherical symmetry. Figure 16 is perhaps most appropriate for nuclei like  $\text{Os}^{188}$  or  $\text{Os}^{190}$ .

## VII. DISCUSSION OF EVIDENCE FOR VIBRATIONAL STATES IN DEFORMED EVEN-EVEN NUCLEI

Until now we have been concerned with the systematization of the levels which qualify because of their spin and parity to be considered as vibrational. In this

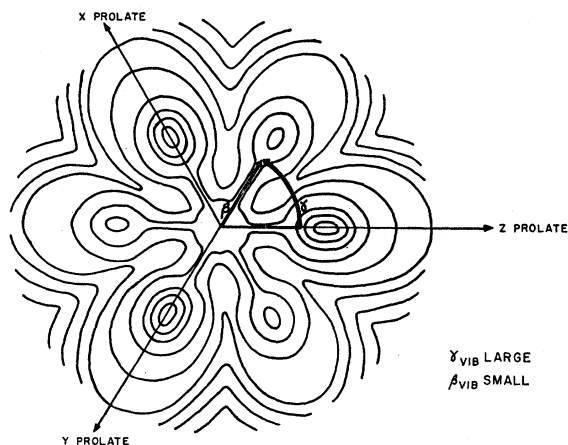


FIG. 14. Contour map of the potential energy diagram of a nucleus which has a relatively low energy  $\beta$  vibration and a relatively high energy  $\gamma$  vibration. This nucleus is approaching the "beta unstable" idealization shown in Fig. 13. Examples from the beginning of a region of deformation are  $\text{Nd}^{150}$ ,  $\text{Sm}^{152}$ ,  $\text{Gd}^{154}$ ,  $\text{Ra}^{222}$ ,  $\text{Ra}^{224}$ ,  $\text{Ra}^{226}$ ,  $\text{Th}^{226}$ , and  $\text{Th}^{228}$ .

section we attempt, first, to summarize this evidence, and second, to adduce additional evidence from the Coulomb-excitation cross sections for these states.

### A. Systematic Occurrences of $0+$ and $2+$ Bands and Existence and Nature of Impurities in These Bands

The systematic occurrence in deformed even-even nuclei of states with  $I=2, K=2$ , and its superimposed rotational band, and states of  $I=0, K=0$ , and its superimposed rotational band is evidence for the collective nature of these states and their consequent classification as  $\gamma$  and  $\beta$  vibrations, respectively, and is summarized in Sec. IV.

In spite of their relatively systematic energy dependence, one is still forced to ask the question, "Do these states have important admixtures of other in-

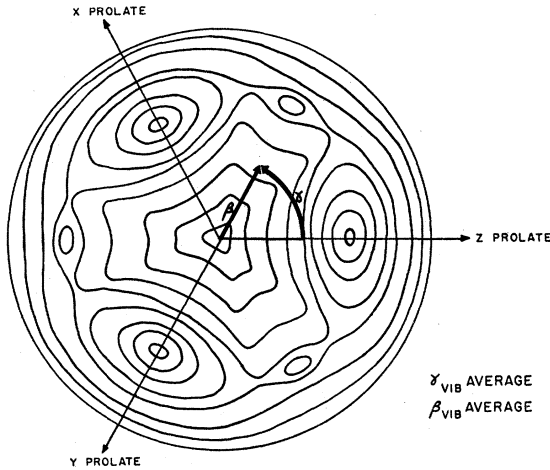


FIG. 15. Contour map of the potential energy diagram of a nucleus which has relatively high energy  $\beta$  and  $\gamma$  vibrations. Many of the nuclei in the middle of the region of deformation have this type of potential energy diagram. An example is  $\text{Pu}^{239}$  (Fig. 3).

trinsic states in their wave functions?" The collective model predicts intensity branching ratios between the vibrational bands and the ground state band. These predictions are predicated upon the purity of the vibrational bands and the ground state band. Small amounts of common impurities in the vibrational and ground state bands will have a large effect on the branching ratios. Therefore, the determination of these branching ratios is a sensitive method of determining certain types of common impurities. Consider, for example, the branching ratio from the  $2+, K=2$  state to the ground state rotational band  $I=0+, 2+, \text{ and } 4+$ . The collective model predicts that the  $B(2, 2 \rightarrow 0, 0)/B(2, 2 \rightarrow 0, 2)$  should be 0.7. The actual experimental value for this branching ratio plotted against  $A$  for a number of nuclei is shown in Figure 17.<sup>23</sup> The experimental branching ratio always falls below the theo-

<sup>23</sup> Hansen, Nielsen, and Sheline, Nuclear Phys. 12, 389 (1959).

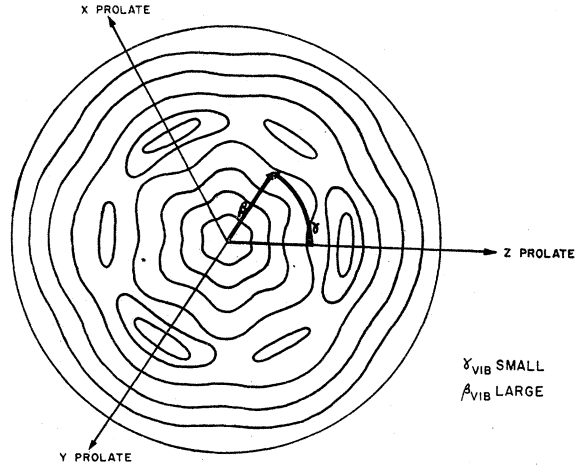


FIG. 16. Contour map of the potential energy diagram of a nucleus which has a relatively low energy  $\gamma$  vibration and a relatively high energy  $\beta$  vibration. Examples from the end of a region of deformation are  $\text{W}^{186}$ ,  $\text{Os}^{188}$ ,  $\text{Os}^{190}$ , and  $\text{Os}^{192}$ .

retical value and approaches most nearly the theoretical value in the middle of the region of deformation. It is possible to interpret these systematic deviations in terms of *small* admixtures of impurity wave functions. One might expect that these are mixtures of  $K=1$  states which lie at considerably higher energies. Such impurity wave functions can change the intensity rules considerably in view of the large transition probabilities within rotational bands.<sup>24</sup>

These systematic deviations can be formulated by introducing a parameter  $z$  describing the interaction between the two bands. If there is no interaction through common impurity wave functions, the reduced transition probability for an  $E2$  transition from a vibrational state with  $K=2$  to the ground state with  $K=0$  can be written

$$B(E2; 2, I_i \rightarrow 0, I_f) = \langle 0 | M(E2, \nu) | 2 \rangle^2 \langle I_i 222 - 2 | I_i 2I_f 0 \rangle^2. \quad (\text{VII.1})$$

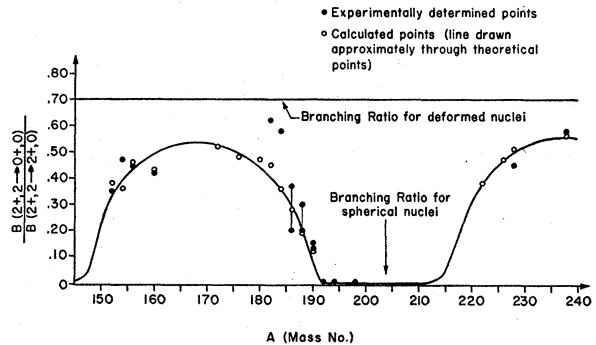


FIG. 17. Plot of the calculated and experimentally determined branching ratios of the transitions from the  $2+, K=2, \gamma$  vibrations to the  $0+, K=0$  and  $2+, K=0$  ground state levels.

<sup>24</sup> Alaga, Alder, Bohr, and Mottelson, Dan. Matt. Fys. Medd. 29, No. 9 (1955).

TABLE VIII. Correction factor,  $f(z, I_i, I_f)$ , for the transition probability between states with  $K=2$  and  $K=0$ .

Initial state $K=2, I_i =$	Final state $K=0, I_f =$	$f(z, I_i, I_f)$
$I-2$	$I$	$(1+2I+1)z^2$
$I-1$	$I$	$(1+(I+2)z)^2$
$I$	$I$	$(1+2z)^2$
$I+1$	$I$	$(1-(I-1)z)^2$
$I+2$	$I$	$(1-(2I+1)z)^2$

When one introduces a coupling of the two bands by the parameter  $z$ , the reduced transition probability becomes

$$B(E2; 2(0)I_i \rightarrow 0(2), I_f) = zB(E2; 2, I_i \rightarrow 0, I_f)f(z, I_i, I_f). \quad (\text{VII.2})$$

Values for the correction factor  $f$  are given in Table VIII.

The parameter  $z$  should be proportional to

$$(\hbar^2/g)/\hbar\omega_\gamma. \quad (\text{VII.3})$$

This can be seen in the following way:

$$z \sim \frac{\langle K=2 | V | K=0 \rangle}{\hbar\omega_\gamma} \left\{ \frac{B(E2; K=0 \rightarrow K=0)}{B(E2; K=2 \rightarrow K=0)} \right\}^{\frac{1}{2}}, \quad (\text{VII.4})$$

where  $\langle \rangle$  is the matrix element connecting the  $K=2$  and the  $K=0$  band.

However, in the hydrodynamical model,

$$\langle K=2 | V | K=0 \rangle \sim (\hbar^2/g)(\hbar\omega_\gamma/C_2)^{\frac{1}{2}}, \quad (\text{VII.5})$$

$$B(E2K=0 \rightarrow K=0) \sim Q_0^2, \quad (\text{VII.6})$$

and

$$B(E2K=2 \rightarrow K=0) \sim (\hbar\omega_\gamma/C_2)Q_0^2, \quad (\text{VII.7})$$

where  $\hbar\omega_\gamma/C_2$  is the zero-point oscillation of the  $\gamma$  vibration,  $C_2$  is the nuclear deformability for the  $\lambda=2$  mode and is related to the surface energy, and  $Q_0$  is the intrinsic quadrupole moment measured with respect to the nuclear axis. If we substitute (VII.5), (VII.6), and (VII.7) in (VII.4), we find (VII.3).

When the value  $z = 2.7(\hbar^2/g)/\hbar\omega_\gamma$  is used, the open circles shown in Fig. 17 are calculated. The line drawn through these calculated points is shown in the figure, but since both  $g$  and  $\hbar\omega_\gamma$  are functions of both  $Z$  and  $N$ , a perfectly smooth curve plotted against  $A$  cannot be expected to result. The agreement between experiment and theory in Fig. 17 is obvious. A complete treatment for a number of levels in  $\text{Gd}^{156}$  studied by the decay of  $\text{Tb}^{156}$  has been attempted. The agreement for the branching ratios for the  $I=2, K=2$  to the ground state band transitions is within experimental error. Perhaps even more rewarding is the agreement within experimental error of the branching ratio for the  $I=3, K=2$  band to the ground state band. Deviations for the branching ratios of a  $K=4$  band are also qualitatively, although not quantitatively, reproduced.

In summary,  $\beta$  and  $\gamma$  vibrational bands occur systematically, and there is evidence for a small but finite admixture of other wave functions in these bands, the amount of impurities being least in the middle of the region of deformation and greatest at the beginning and especially at the end of the region of deformation.

## B. Coulomb-Excitation Cross Sections to Vibrational States in Deformed Nuclei

It has been recognized for some time that Coulomb excitation represents a particularly powerful method of studying collective excitations. Thus, the nuclear states most strongly produced in Coulomb-excitation reactions are collective excitations induced by the electric quadrupole field of particles passing in the vicinity of the nuclei. Although this method has been used frequently in the study of low-lying rotational states, it has been applied very little in the study of vibrational states of deformed nuclei. Because of the much higher energy of these vibrations, it is experimentally much more difficult to observe them in Coulomb excitation. Nonetheless, Barloutand, Lehmann, and Leveque<sup>25</sup> and McGowan and Stelson<sup>26</sup> have studied a number of Coulomb excitations of vibrational bands. These data are summarized in Table IX.

TABLE IX. Coulomb-excitation cross sections for  $\gamma$  vibrational states (see reference 25).

Nucleus	$E$ of $\gamma$ vib (kev)	$B(E2)$ in s.p. units
$\text{W}^{184}$	$891 \pm 9$	$5.5 \pm 1.6$
$\text{W}^{186}$	$730 \pm 7$	$5.5 \pm 1.0$
$\text{Os}^{188}$	$633 \pm 6$	$6.3 \pm 1.9$
$\text{Os}^{190}$	$557 \pm 6$	$5.3 \pm 1.0$
$\text{Os}^{192}$	$489 \pm 5$	$4.6 \pm 1.0$

The Coulomb excitation of a  $2+$  level at 760 kev in  $\text{Th}^{232}$  has also been reported by McGowan.<sup>27</sup> This level, which is supposed to be the  $2+$  member of the  $\beta$  vibrational band, has a reduced transition probability 4.3 times the single-particle value. All of these measurements of the Coulomb-excitation cross section are indirect since they involve a  $\gamma$ -ray yield after proton bombardment.

More recently a direct measurement of the Coulomb-excitation cross sections has been made on the  $2+$  states of the  $\beta$  and  $\gamma$  bands in  $\text{Sm}^{152}$ . The results are shown in Fig. 18. The measurements<sup>28</sup> were made by utilizing a photographic recording heavy-particle spectrometer to record inelastically scattered particles. In this way, the cross section for excitation of the vibrational states can be obtained directly. Since the cross section for the Rutherford scattering to the ground

<sup>25</sup> Barloutand, Lehmann, and Leveque, *Compt. rend.* **245**, 523 (1957).

<sup>26</sup> F. K. McGowan and P. H. Stelson, *Bull. Am. Phys. Soc.* **II** **3**, 228 (1958).

<sup>27</sup> F. K. McGowan, Report on the Paris Conference (1958).

<sup>28</sup> Shelin, Nielsen, and Sperduto (submitted for publication).

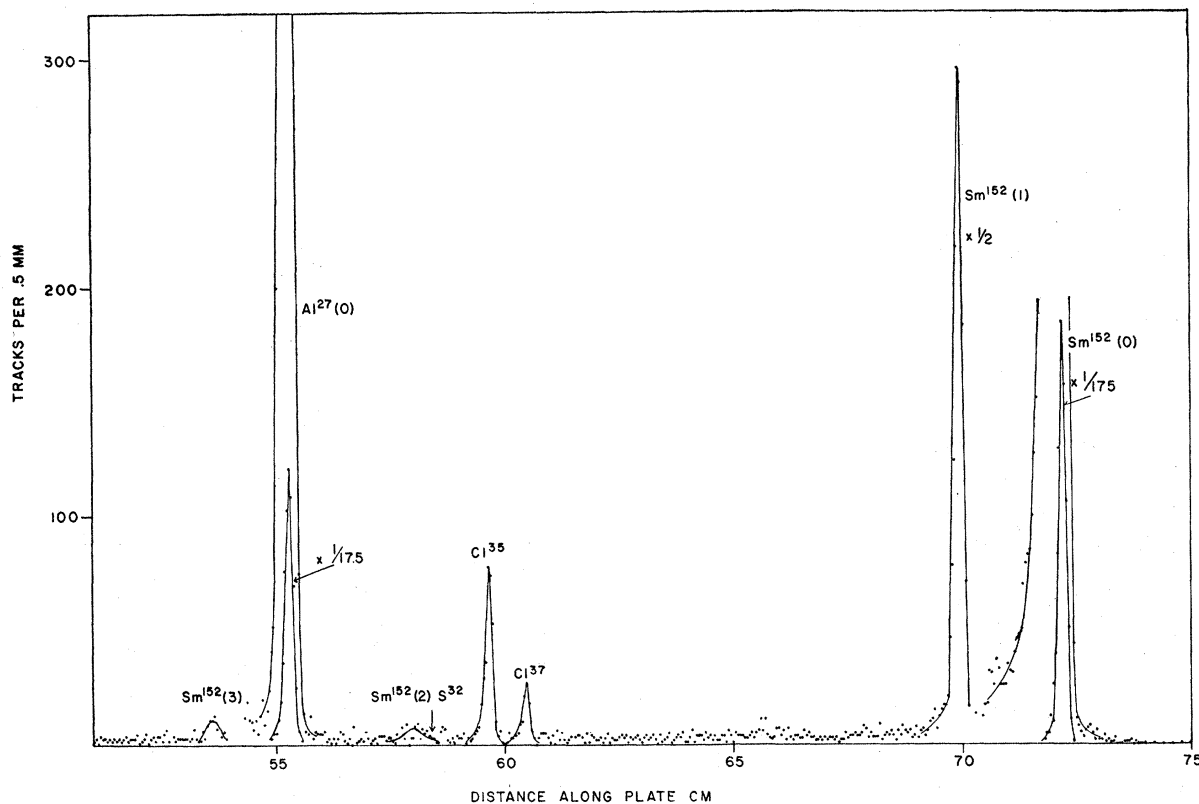


FIG. 18. Elastic and inelastic scattered deuteron groups from a 99.9+%  $\text{Sm}^{152}$  target on aluminized-formvar backing. The exposures were 1750 and 10 microcoulombs. Incident deuteron energy was 8.52 Mev, deflecting angle,  $90^\circ$ . Arrow shows theoretical position of the  $\text{S}^{32}$  elastic scattering peak if sulfur were present in the target.  $\text{Cl}^{36}$  and  $\text{Cl}^{37}$  are the only contaminants detected besides carbon, nitrogen, oxygen, and aluminum from the backing material.

state is well known, the ratios of the intensities of the elastic groups corresponding to the  $\gamma$  and  $\beta$  level excited to that of the elastic group determines the Coulomb-excitation cross section of the vibrational levels. Cross sections determined in this way are independent of a knowledge of conversion coefficients and branching ratios.

As shown in Fig. 18, the excitation cross sections give definite evidence for the existence of levels at 807 and 1079 kev. These energies correspond very closely to  $2+$  levels assigned as  $\beta$  and  $\gamma$  vibrational bands, respectively, in decay scheme studies. Since the measurements are direct ratios, the cross sections determined are extremely reliable within the statistics of the determination. Unfortunately, the statistics are not very good. The differential cross section for the  $2+$   $\beta$  vibration in mb/steradian is 0.06; for the  $2+$   $\gamma$  vibration it is 0.08. This corresponds to reduced transition probabilities of  $0.07 \pm 0.02$  and  $0.12 \pm 0.02$ , respectively, in units of  $e^2 \times 10^{-48} \text{ cm}^4$  or  $3 \pm 1$  and  $5 \pm 1$  in single-particle units. This is strong evidence that both the  $\beta$  and  $\gamma$  vibrations in  $\text{Sm}^{152}$  have a considerable collective character. Whereas rotational cross sections indicate lifetimes of the order of  $10^2$  times faster than the corresponding single-particle lifetimes, the lifetime of these

states is only a few times the lifetime of the corresponding single-particle states.

### C. Evidence from the Vibrational States in Spherical Nuclei

In the introduction, evidence supporting the assignments of certain levels in the spherical nuclei as vibrational was presented. We have shown very clearly in the systematics of levels that both at the beginning and at the end of the regions of deformation the  $\beta$  and  $\gamma$  bands connect smoothly to the states in spherical nuclei which the experimental evidence supports as vibrational. We may use this relationship as additional evidence in support of the vibrational character of the  $\beta$  and  $\gamma$  bands in deformed nuclei.

### D. Selection Rules and Other Characteristics of Vibrational States in Deformed Nuclei

In spherical even-even nuclei, one of the evidences for vibrational states is the observation that the transition from the second to the first  $2+$  state is largely  $E2$  although the shell model would predict that  $M1$  transitions should be about 500 times stronger than  $E2$  transitions.<sup>2</sup> Deformed even-even nuclei also have

transitions from the second to the first  $2+$  states which are largely  $E2$ . However, the selection rule applied generally against  $M1$  transitions in spherical nuclei must be applied cautiously in deformed nuclei. Usually, the second  $2+$  state in deformed nuclei is the  $K=2$ ,  $I=2+$   $\gamma$  vibration. The transition from this state to the first excited  $K=0$ ,  $I=2+$  state will have  $E2$  character because<sup>24</sup>  $|K_i - K_f| \Delta K \leq L$ .

In this case, consequently, the  $E2$  character is accounted for by the  $K$  selection rule and is therefore not evidence for a vibration. On the other hand, a transition from a  $K=0$ ,  $I=2+$   $\beta$  vibration to the  $K=0$ ,  $I=2+$  first excited state would not be expected purely on the basis of the  $K$  selection rule to have  $E2$  character. The fact that these transitions are also largely  $E2$  in character<sup>29</sup> in  $Gd^{164}$  and  $Sm^{152}$  is strong evidence for their classification as vibrations. It further suggests the possibility of a study in which the relative amount of  $E2$  to  $M1$  is compared in transitions between  $\gamma$  states with  $n_\gamma=1$ ,  $n_\beta=0$ ,  $K=2$ ,  $I=2$  and ground state bands with  $n_\gamma=0$ ,  $n_\beta=0$ ,  $K=0$ ,  $I=2$  and between  $\beta$  bands with  $n_\gamma=0$ ,  $n_\beta=1$ ,  $K=0$ ,  $I=2$  and the ground state bands. In this way it might be possible to separate that part of the increased  $E2$  transition probability, in the more common  $\gamma$  state  $K=2$ ,  $I=2$  which decays to the ground  $K=0$ ,  $I=2$  state, which is due to the  $K$  selection rules and that part which is due to the vibrational selection rule.

A second characteristic of vibrational states should be a regular spacing between 1, 2, 3,  $\dots$  phonon states. Thus, for example,

$$E_{n_\gamma=0, n_\beta=2} / E_{n_\gamma=0, n_\beta=1} \quad \text{and} \quad E_{n_\gamma=2, n_\beta=0} / E_{n_\gamma=1, n_\beta=0}$$

should be approximately two or, if we follow the lead of the spherical region, 2.2. Unfortunately, there is very little data with which to test this expected characteristic of vibrational states. The two-phonon states often lie too high in energy to be distinguished easily from the complexity of intrinsic and rotational states. Those regions which offer the greatest opportunity for observing two-phonon states are the beginning and ends of the regions of deformation. Thus, for example, a two-phonon  $\beta$  vibration with  $n_\beta=2$ ,  $n_\gamma=0$ ,  $K=0$ ,  $I=0$  is to be expected at  $\sim 1500$  keV in  $Nd^{150}$ ,  $Sm^{152}$ , and  $Gd^{164}$ . Similarly, a two-phonon  $\gamma$  vibration with  $n_\gamma=2$ ,  $n_\beta=0$ ,  $K=0$  and 4, and  $I=0$  and 4 is to be expected at  $\sim 1390$  keV in  $Os^{188}$  and  $\sim 1225$  keV in  $Os^{190}$ .

$0+$  states have been observed in  $Os^{188}$  at 1086 and 1765 keV.<sup>30</sup> There is some evidence that these states are mixed, both having some of the character of the  $n_\gamma=2$ , two-phonon state. If, therefore, as a first approximation we average the energy of these states, we get the value 1426 keV in excellent agreement with 1390

keV. Nielsen *et al.*<sup>31</sup> have found a state at 1161 keV in  $Os^{190}$  which has spin  $2+$ ,  $3+$ , or  $4+$  and may correspond with the  $n_\gamma=2$ ,  $n_\beta=0$ ,  $K=4$  state (see Fig. 19). The ratio of the energies of the  $n_\gamma=2$  and  $n_\gamma=1$  states is 2.08.

A final criterion in testing for vibrational states is the probable existence of certain selection rules involving the quantum numbers  $n_\gamma$  and  $n_\beta$ . Since we have essentially independent oscillations in the  $\beta$  and  $\gamma$  variables, the selection rules involving  $n_\beta$  and  $n_\gamma$  are also independent. Descriptively, the selection rule says that in a transition involving different vibrational states, the change in  $n_\beta$  must be one and/or the change in  $n_\gamma$  must be one. Other transitions involving different vibrational states should be forbidden. Analytically stated,

$$\Delta n_\beta = 1 \quad \text{and/or} \quad \Delta n_\gamma = 1.$$

Deviations in the wave functions implying that  $n_\beta$  and  $n_\gamma$  are not exact constants of the motion relax this selection rule. This tends to retard rather than completely forbid the transition. We refer to such transitions as  $\beta$ -forbidden,  $\gamma$ -forbidden, or  $\beta\gamma$ -forbidden depending on whether  $\Delta n_\beta$ ,  $\Delta n_\gamma$ , or both  $\Delta n_\beta$  and  $\Delta n_\gamma$  selection rules are involved. The degree of forbiddenness is  $\Delta n_\beta - 1$  for  $\beta$ -forbiddenness,  $\Delta n_\gamma - 1$  for  $\gamma$ -forbiddenness, and  $\Delta n_\beta + \Delta n_\gamma - 2$  for  $\beta\gamma$ -forbiddenness.

A possible test for these selection rules is provided in the  $\gamma$ -forbiddenness in transitions involving  $\Delta n_\gamma=2$  in  $Os^{188}$  and  $Os^{190}$ . Thus, each of the two  $0+$  states in  $Os^{188}$  decays with measured intensities<sup>32</sup> to both the  $n_\gamma=1$ ,  $2+$  state at 633 keV and the  $n_\gamma=0$  state at 155 keV. The ratio of the transition probability to these two states (assuming that each transition is pure  $E2$ ) provides an approximate determination of the magnitude of this  $\gamma$ -forbiddenness.

For the 1765-keV state,

$$\begin{aligned} & B(E2) \text{ 1765} \rightarrow 633 \\ & \hline & B(E2) \text{ 1765} \rightarrow 155 \\ & = \left( \frac{1610}{1132} \right)^5 \frac{0.07\% \langle 0202 | 0222 \rangle^2}{0.07\% \langle 0200 | 0220 \rangle^2} = 5.8. \quad (\text{VII.1}) \end{aligned}$$

For the 1086-keV state,

$$\begin{aligned} & B(E2) \text{ 1086} \rightarrow 633 \\ & \hline & B(E2) \text{ 1086} \rightarrow 155 \\ & = \left( \frac{931}{454} \right)^5 \frac{0.04\% \langle 0202 | 0222 \rangle^2}{0.41\% \langle 0200 | 0220 \rangle^2} = 3.7. \quad (\text{VII.2}) \end{aligned}$$

This seems to indicate that both the 1086- and the 1765-keV states have some of the forbiddenness asso-

<sup>29</sup> O. Nathan (private communication).

<sup>30</sup> Marklund, Van Nooijen, and Grabowski, reported at the Annual Meeting of the Swedish Physical Society (June, 1959); Nathan, Nilsson, and Bes (private communication).

<sup>31</sup> Nielsen, Poulsen, Sheline, and Jensen, Nuclear Phys. **10**, 485 (1959).

<sup>32</sup> Johns, McMullen, Williams, and Nablo, Can. J. Phys. **34**, 69 (1956).



accuracy. This is necessary if one is to use the deviations from the  $I(I+1)$  energy dependents in the ground state band to determine the position of vibrational levels, (2) that the search for additional  $\gamma$  and  $\beta$  vibrational bands should continue, (3) that measurements of branching ratios from vibrational bands to the ground state bands to determine the purity of the involved states is important, (4) that comparison of the experimentally measured moments of inertia of ground state bands and  $\beta$  and  $\gamma$  vibrational bands is important, (5) that measurement of Coulomb-excitation cross sections of vibrational bands in both odd  $A$  and even-even nuclei should continue, (6) that observation of the relative amount of  $E2$  character in transitions from the  $2+$  states of both  $\beta$  and  $\gamma$  vibrational bands to the  $2+$  states of the ground state band be continued, (7) that a search be made for additional two-phonon states ( $n_\beta=2, n_\gamma=0$  and  $n_\beta=0, n_\gamma=2$ ) and a study of their energies relative to their respective one-phonon states be made, and (8) that a careful study of the decay of two-phonon states be undertaken to determine if there are  $\Delta n_\beta$ ,  $\Delta n_\gamma$ , and  $\Delta n_\beta \Delta n_\gamma$  selection rules for vibrations.

Accumulation of such data will probably give increasing evidence for the existence of vibrational bands in deformed nuclei. Simultaneously, it will define the degree of independence of these vibrations from rotations and intrinsic configurations. Most certainly it will show some of the predictions and relationships presented here to be in error. The very nature of this paper, in

trying to move so far ahead of experiment in a field which has been bound so closely to experiment, implies this. It is to be hoped that some of the predictions and relationships presented here will stand the test of experiment and that the errors may often be understood in terms of refinements of ideas herein presented.

In any case, the field of nuclear vibrations is a challenging one for both experimentalists and theorists.

#### IX. ACKNOWLEDGMENTS

This work was initiated during the summer of 1956 at the Institute for Theoretical Physics in Copenhagen. The excellent working facilities provided by Professor Niels Bohr are gratefully acknowledged. The stimulation of the nuclear chemistry and  $\beta$ -spectroscopy groups, particularly civil engineers Sven Bjornholm, P. Gregers Hansen, Skytte Jensen, Ove Nathan, and O. B. Nielsen, were of great value. Of particular importance were discussions with Professor Aage Bohr and Professor B. R. Mottelson. More recently, most of the data has been reworked, additional data have been added, and the paper written at Florida State University in Tallahassee, Florida. Thanks are due Professor Aage Bohr and Mr. Daniel Bes for critically reading this manuscript. Completion was aided by contracts with the Office of Ordnance Research, (DA-01-009-ORD-705) and the U. S. Atomic Energy Commission (AT-(40-1)-2434). The stimulation of civil engineer Henrik Loft Nielsen was also of considerable importance.